Award Number: W81XWH-12-1-0622

TITLE: Assessment of Biomarkers Associated with Joint Injury and Subsequent Post-Traumatic Arthritis

PRINCIPAL INVESTIGATOR: Virginia B. Kraus

CONTRACTING ORGANIZATION: Duke University
Durham, NC 27705

REPORT DATE: October 2015

TYPE OF REPORT: Annual

PREPARED FOR: U.S. Army Medical Research and Materiel Command
Fort Detrick, Maryland 21702-5012

REPORT DOCUMENTATION PAGE

Form Approved
OMB No. 0704-0188

1. REPORT DATE	**2. REPORT TYPE**	**3. DATES COVERED**
October 2015	Annual	30 Sep 2014 - 29 Sep 2015

4. TITLE AND SUBTITLE

Assessment of Biomarkers Associated with Joint Injury and Subsequent Post-Traumatic Arthritis

5a. CONTRACT NUMBER
OR110100P1

5b. GRANT NUMBER
W81XWH-12-1-0622

5c. PROGRAM ELEMENT NUMBER

6. AUTHOR(S)

Steven A. Olson, Farshid Guilak, Virginia B. Kraus, Bridgette D. Furman, Kelly A. Kimmerling, Janet L. Huebner, Louis E. DeFrate

E-Mail: vbk@duke.edu

5d. PROJECT NUMBER

5e. TASK NUMBER

5f. WORK UNIT NUMBER

7. PERFORMING ORGANIZATION NAME(S) AND ADDRESS(ES)

Duke University
School of Medicine
2200 West Main St.
Suite 820 Erwin Square Plaza
Durham, NC 27705

8. PERFORMING ORGANIZATION REPORT NUMBER

9. SPONSORING / MONITORING AGENCY NAME(S) AND ADDRESS(ES)
U.S. Army Medical Research and Materiel Command
Fort Detrick, Maryland 21702-5012

10. SPONSOR/MONITOR'S ACRONYM(S)

11. SPONSOR/MONITOR'S REPORT NUMBER(S)

12. DISTRIBUTION / AVAILABILITY STATEMENT
Approved for Public Release; Distribution Unlimited

13. SUPPLEMENTARY NOTES

14. ABSTRACT
The overall objective of this research effort is to identify biomarkers following articular fracture that may be predictive of the development of post-traumatic arthritis (PTA). PTA is a clinically important complication of joint injury with life-long effects for the patient. While PTA can occur rapidly after moderate to severe articular injuries, not every patient will go on to develop this condition. There are no effective screening methods to determine who is at risk. This proposal includes both a clinical observational study and a series of murine experiments, both with the goal of identifying biomarkers that are associated with development of PTA. Patients with knee joint fractures will be enrolled, and we will collect serum, urine, and synovial fluid early after injury. Radiographic imaging will be performed early after injury, again at 18 months, and analyzed to determine which patients developed PTA from those who did not. We will assess the ability of identified biomarkers in serum, urine, and synovial fluid to predict PTA following joint injury. Additionally, biomarkers will be assessed in a murine model of articular fracture using two strains in which one strain develops PTA and the other does not. Comparison of the human and mouse response to knee joint fracture will allow assessment of the potential use of the mouse model to evaluate future therapies to prevent PTA.

15. SUBJECT TERMS

Nothing listed

16. SECURITY CLASSIFICATION OF:			**17. LIMITATION OF ABSTRACT**	**18. NUMBER OF PAGES**	**19a. NAME OF RESPONSIBLE PERSON**
a. REPORT	**b. ABSTRACT**	**c. THIS PAGE**			USAMRMC
U	U	U	UU	35	**19b. TELEPHONE NUMBER** *(include area code)*

Table of Contents

Page

Introduction…….. 4

Body…….. 4

Key Research Accomplishments…….. 16

Conclusion…… 16

Reportable Outcomes…… 17

References…… 17

Tables…… 19

Appendices…… 21

"Assessment of Biomarkers Associated with Joint Injury and Subsequent Post-Traumatic Arthritis"
Start date: 9/30/2012
PIs – Steven A. Olson **(SAO)**; Farshid Guilak **(FG)**; and Virginia B Kraus **(VBK)**

1. INTRODUCTION:

Post-traumatic arthritis (PTA) is a clinically important complication of joint injury with life-long effects for the patient.[1,2] PTA is a severe burden in active duty and discharged soldiers.[3] While PTA can occur rapidly after moderate to severe articular injuries, not every patient will go on to develop this condition. There are no effective screening methods to determine who is at risk for developing PTA. The overall objective of this proposal is to identify biomarkers following articular fracture that may be predictive of the development of PTA. To accomplish this we will conduct a two-part study. We will perform a prospective observational study of patients with lower extremity articular fractures requiring operative treatment. Patients with knee joint fractures will be enrolled, and we will collect serum, urine, and synovial fluid from each patient acutely after injury. Radiographic imaging will be performed early after injury and again at 18 months. Both scans will be analyzed to separate the patients that developed PTA from those who did not. We will assess the ability of identified biomarkers in serum, urine, and synovial fluid to predict PTA following joint injury. Additionally, biomarkers will be assessed in a murine model of articular fracture using two strains in which one strain develops PTA and the other does not. Comparison of the human and mouse response to knee joint fracture will allow for assessment of the potential use of the mouse model to evaluate future therapies to prevent PTA. The low cost of mouse models lends itself to this type of work, and the results will provide a validated model to use for studying PTA. The goal of this work is to establish the basis for future use of biomarkers to predict the potential risk for developing PTA after acute joint injury. In addition, this work will elucidate data on biospecimens that may be useful in future registries of acute joint injuries.

2. KEYWORDS:

Post-traumatic arthritis, post-traumatic osteoarthritis, articular fracture, joint injury, trauma, biomarker, inflammation, MRI, knee, mouse model, translational research.

3. OVERALL PROJECT SUMMARY:

The overall objective of this study is to identify biomarkers following articular fracture that may be predictive of the development of PTA. Specifically, patients with a closed unilateral articular fracture of the knee requiring operative treatment will be enrolled over an 18-month period. Biosamples (synovial fluid from the injured and contralateral uninjured knee, serum, and urine) will be collected prior to or at surgical intervention. MRI imaging of the injured knee will be obtained to assess the articular cartilage. Degenerative changes in the cartilage and joint space narrowing will be correlated to biomarkers that may be indicative and predictive of joint degeneration and the development of PTA. We have successfully enrolled patients, collected and stored biosamples, obtained all post-operative MRI scans and are continuing to obtain 18-month MRI scans for study patients. Enrollment was initially slow. However, we addressed this issue by expanding the enrollment criteria and have received a one year no cost extension in order to complete all analyses. Sample collection and processing has been very successful, and we are pleased with the quantity of biosamples collected and MRI analyses.

The second aim of this study is to create closed tibial plateau fractures in the left knee of C57BL/6 mice that develop PTA and MRL/MpJ mice that are protected from PTA. Serum and synovial fluid will be collected from both strains at various time points. Biospecimens will be analyzed for markers of joint inflammation and degradation identified in the human knee following articular injury. Biomarkers will be correlated to joint pathology that will be assessed

from microCT and histology. The human and mouse biomarker profiles associated with PTA will be compared to assess correlations between them. We have successfully completed the short-term data collection (pre-fracture, 0, 1, 7 and 14 days post-fracture), including receiving animals, fracturing, sacrificing, and collection of biosamples. MicroCT and histologic analyses have also been completed for the short-term cohort. We have successfully completed the long-term data collection (8 weeks post-fracture), including receiving the animals, fracturing, sacrificing, and collection of biosamples. MicroCT and histologic analyses are completed.

The details of our progress to date are described below with each task outlined from the approved Statement of Work (SOW).

A. SPECIFIC AIM 1: TASKS

Task 1. Review and approval of IRB protocol (months 1-4) **[SAO, VBK] COMPLETED**

- Duke IRB application submitted on 05/31/2012
- Duke IRB application approved on 07/11/2012
- Amendment to Duke IRB protocol to expand enrollment criteria submitted on 05/06/2013
- Amendment to Duke IRB protocol to expand enrollment criteria approved on 05/17/2013

Task 2. USAMRMC Office of Research Protections review and approval of human use documents (months 1-6) **[SAO] COMPLETED**

- IRB application submitted to USAMRMC Office of Research Protections for review on 09/06/2012
- IRB application approved by USAMRMC Office of Research Protections on 09/21/2012
- Request to expand enrollment criteria was submitted with prior progress report on 04/09/2013
- Response from USAMRMC ORP HRPO received on 05/02/2013.
    - We were informed that the expanded enrollment criteria was not a substantive modification/amendment to our protocol and does not increase risk to subjects. Therefore, the only action needed was to amend the protocol and submit to our Duke IRB for expedited review/approval.

Task 3. Enroll 30 patients in study (months 4-18) **[SAO, FG, VBK] COMPLETED**

3a. Patients with closed unilateral articular fracture of the knee requiring operative treatment will be enrolled in study

3b. Biosamples (synovial fluid, blood, urine) will be collected at time of placing a temporizing spanning external fixator

- First patient enrolled on 12/19/2012 **[SAO]**
    - Synovial fluid, blood, urine processed and stored in -80° freezer **[FG, VBK]**
- Second patient enrolled on 03/06/2013 **[SAO]**
    - Synovial fluid, blood, urine processed and stored in -80° freezer **[FG, VBK]**
- Third patient enrolled on 06/19/2013 **[SAO]**
    - Synovial fluid, blood, urine processed and stored in -80° freezer **[FG, VBK]**
- Fourth patient enrolled on 07/03/2013 **[SAO]**
    - Synovial fluid, blood, urine processed and stored in -80° freezer **[FG, VBK]**
- Fifth patient enrolled on 07/18/2013 **[SAO]**
    - Synovial fluid, blood, urine processed and stored in -80° freezer **[FG, VBK]**
- Sixth patient enrolled on 07/23/2013 **[SAO]**
    - Synovial fluid, blood, urine processed and stored in -80° freezer **[FG, VBK]**
- Seventh patient enrolled on 07/25/2013 **[SAO]**
    - Synovial fluid, blood, urine processed and stored in -80° freezer **[FG, VBK]**
- Eighth patient enrolled on 08/23/2013 **[SAO]**
    - Synovial fluid, blood, urine processed and stored in -80° freezer **[FG, VBK]**

- Ninth patient enrolled on 09/12/2013 **[SAO]**
  - Synovial fluid, blood, urine processed and stored in -80° freezer **[FG, VBK]**
- Tenth patient enrolled on 10/29/2013 **[SAO]**
  - Synovial fluid, blood, urine processed and stored in -80° freezer **[FG, VBK]**
- Eleventh patient enrolled on 05/21/2014 **[SAO]**
  - Synovial fluid, blood, urine processed and stored in -80° freezer **[FG, VBK]**
- Twelfth patient enrolled on 05/29/2014 **[SAO]**
  - Synovial fluid, blood, urine processed and stored in -80° freezer **[FG, VBK]**
- Thirteenth patient enrolled on 06/05/2014 **[SAO]**
  - Synovial fluid, blood, urine processed and stored in -80° freezer **[FG, VBK]**
- Fourteenth patient enrolled on 06/10/2014 **[SAO]**
  - Synovial fluid, blood, urine processed and stored in -80° freezer **[FG, VBK]**
- Fifteenth patient enrolled on 06/25/2014 **[SAO]**
  - Synovial fluid, blood, urine processed and stored in -80° freezer **[FG, VBK]**
- Sixteenth patient enrolled on 06/19/2014 **[SAO]**
  - Synovial fluid, blood, urine processed and stored in -80° freezer **[FG, VBK]**
- Seventeenth patient enrolled on 09/04/2014 **[SAO]**
  - Synovial fluid, blood, urine processed and stored in -80° freezer **[FG, VBK]**
- Eighteenth patient enrolled on 09/25/2014 **[SAO]**
  - Synovial fluid, blood, urine processed and stored in -80° freezer **[FG, VBK]**
- Synovial fluid, blood, urine processed and stored in -80° freezer **[FG, VBK]**
  - 19th patient enrolled on 12/3/2014 **[SAO]**
- Synovial fluid, blood, urine processed and stored in -80° freezer **[FG, VBK]**
  - 20th patient enrolled on 12/4/2014 [SAO]
- Synovial fluid, blood, urine processed and stored in -80° freezer **[FG, VBK]**
  - Enrollment closed **[SAO]**

*Task 4. V*isual analog pain score, the Knee injury and Osteoarthritis Outcome Score (KOOS), and the SF-36 will be completed within 2 weeks of injury. **[SAO] COMPLETED**

- Visual analog pain score, KOOS, and SF-36 for first patient was completed on 12/27/2012 **[SAO]**
- Visual analog pain score, KOOS, and SF-36 for second patient was completed on 03/06/13 **[SAO]**
- Visual analog pain score, KOOS, and SF-36 for third patient was completed on 06/20/2013 **[SAO]**
- Visual analog pain score, KOOS, and SF-36 for fourth patient was completed on 07/01/2013 **[SAO]**
- Visual analog pain score, KOOS, and SF-36 for fifth patient was completed on 07/17/2013 **[SAO]**
- Visual analog pain score, KOOS, and SF-36 for sixth patient was completed on 07/22/2013 **[SAO]**
- Visual analog pain score, KOOS, and SF-36 for seventh patient was completed on 07/23/2013 **[SAO]**
- Visual analog pain score, KOOS, and SF-36 for eighth patient was completed on 08/23/2013 **[SAO]**
- Visual analog pain score, KOOS, and SF-36 for ninth patient was completed on 09/13/2013 **[SAO]**
- Visual analog pain score, KOOS, and SF-36 for ninth patient was completed on 09/13/2013 **[SAO]**
- Visual analog pain score, KOOS, and SF-36 for tenth patient was completed on 10/31/2013 **[SAO]**

- Visual analog pain score, KOOS, and SF-36 for eleventh patient was completed on 05/20/2014 **[SAO]**
- Visual analog pain score, KOOS, and SF-36 for twelfth patient was completed on 05/21/2014 **[SAO]**
- Visual analog pain score, KOOS, and SF-36 for thirteenth patient was completed on 05/28/2014 **[SAO]**
- Visual analog pain score, KOOS, and SF-36 for fourteenth patient was completed on 06/09/2014 **[SAO]**
- Visual analog pain score, KOOS, and SF-36 for fifteenth patient was completed on 06/13/2014 **[SAO]**
- Visual analog pain score, KOOS, and SF-36 for sixteenth patient was completed on 06/20/2014 **[SAO]**
- Visual analog pain score, KOOS, and SF-36 for seventeenth patient was completed on 09/02/2014 **[SAO]**
- Visual analog pain score, KOOS, and SF-36 for eighteenth patient was completed on 09/22/2014 **[SAO]**
- Visual analog pain score, KOOS, and SF-36 for nineteenth patient was completed on 11/25/2014 **[SAO]**
- Visual analog pain score, KOOS, and SF-36 for twentieth patient was completed on 12/04/2014 **[SAO]**

Task 5. Biosamples (synovial fluid, blood, urine) will be collected at time of definitive fixation of closed unilateral articular fracture of the knee requiring operative treatment. Timing of repair will be based on standard of care for treating the clinical injury. **[SAO, FG, VBK] COMPLETED**

- Biosamples from first patient collected at time of definitive fixation on 12/22/2012 **[SAO]**
  - Synovial fluid, blood, urine processed and stored in -80° freezer **[FG]**
- Biosamples from second patient collected at time of definitive fixation on 3/13/2013 **[SAO]**
  - Synovial fluid, blood, urine processed and stored in -80° freezer **[FG]**
- Patients 3 – 9 had definitive fixation at the baseline visit so a second set of biosamples was not collected. **[SAO]**
- Biosamples from the 10th patient collected at time of definitive fixation on 11/12/2013 **[SAO]**
  - Synovial fluid, blood, urine processed and stored in -80° freezer **[FG]**
- Biosamples from the 14th patient collected at time of definitive fixation on 6/17/2014 **[SAO]**
  - Synovial fluid, blood, urine processed and stored in -80° freezer **[FG]**
- Patients 11-13 and 15-20 had definitive fixation at the baseline visit so a second set of biosamples was not collected. **[SAO]**

Task 6. Post-operative follow-up of all patients (months 5-18) **[SAO]**

6a. Post-operative T1-rho MRI will be obtained

6b. Analysis of MRI T1-rho imaging of cartilage

- Post-operative MRI obtained from first patient on 01/30/2013 **[SAO]**
- Post-operative MRI obtained for second patient on 04/30/2013 **[SAO]**
- Post-operative MRI attempted for third patient on 08/06/2013; patient experienced claustrophobia associated with the MRI machine and may not return to study **[SAO]**
- Post-operative MRI not obtained for fourth patient because patient will have a total knee replacement; patient does not satisfy enrollment criteria and has been removed from the study **[SAO]**
- Post-operative MRI obtained for fifth patient on 11/01/2013 **[SAO]**
- Post-operative MRI obtained for sixth patient on 09/23/2013 **[SAO]**

- Post-operative MRI obtained for seventh patient on 09/26/2013 **[SAO]**
- Post-operative MRI not obtained for eighth patient because definitive fixation resulted in just an external fixation; patient does not satisfy enrollment criteria and has been removed from the study **[SAO]**
- Post-operative MRI obtained for ninth patient on 10/28/2013; patient withdrew from study so no further MRI will be obtained **[SAO]**
- Post-operative MRI obtained for tenth patient on 01/14/2014 **[SAO]**
- Post-operative MRI obtained for eleventh patient on 07/16/2014 **[SAO]**
- Post-operative MRI not obtained for twelfth patient; patient has been withdrawn from study due to non-compliance **[SAO]**
- Post-operative MRI not obtained for thirteenth patient; patient has been withdrawn from study due to non-compliance **[SAO]**
- Post-operative MRI obtained for fourteenth patient on 08/11/2014 **[SAO]**
- Post-operative MRI obtained for fifteenth patient on 08/15/2014 **[SAO]**
- Post-operative MRI obtained for sixteenth patient on 09/16/2014 **[SAO]**
- Post-operative MRI scheduled for seventeenth patient on 11/03/2014 **[SAO]**
- Post-operative MRI scheduled for eighteenth patient on 11/07/2014 **[SAO]**
- Post-operative MRI obtained for 19th patient on 3/6/2015 **[SAO]**
- Post-operative MRI obtained for 20th patient on 7/7/2015 **[SAO]**
- Review and analysis of MRI scans is underway for assessment of cartilage **[SAO]**

Task 7. 18-month follow-up of all patients (months 19-36) [SAO]

- 18-month follow-up MRI obtained for first patient on 07/10/2014 **[SAO]**
- 18-month follow-up MRI obtained for second patient on 09/24/2014 **[SAO]**
- 18-month follow-up MRI for 5th patient obtained on 2/4/2015 **[SAO]**
- 18-month follow-up MRI for 6th patient obtained on 3/25/2015 **[SAO]**
- 18-month follow-up MRI for 7th patient obtained on 3/23/2015 **[SAO]**
- 18-month follow-up MRI for 10th patient is questionable as the patient has moved out of the area, but the clinical research coordinator continues to attempt to contact. **[SAO]**
- 18-month follow-up MRI for 11th patient is scheduled for 11/19/2015 **[SAO]]**
- 18-month follow-up MRI for patients 14,15 and 16 will be scheduled over the next quarter **[SAO]**
- 18-month follow-up MRI for patients 3-4, 8-9, and 12-13 will not obtained for reasons listed in Task 6 **[SAO]**
- Review and analysis of MRI scans is underway for assessment of cartilage **[SAO]**

Task 8. Perform assays of biosamples to assess acute levels of inflammatory and injury markers (months 18-30) **[VBK]**

- All samples have been transferred to Kraus lab **[FG, VBK]**
- Selection of markers and assay panels has been completed **[VBK]**
- Serum and synovial fluid assayed using inflammatory and injury multiplex array **[VBK]**

Task 9. Submit samples for proteomics analysis (months 24-30) [**SAO** assisted by **VBK**]

- All samples have been transferred to Kraus lab **[SAO, FG, VBK]**
- Selection of targeted proteomics and discovery metabolomics has been completed **[VBK, SAO]**
- Serum samples submitted for targeted proteomic panel completed and awaiting statistical analyses **[VBK]**
- Synovial fluid samples to be submitted for discovery metabolomics in next quarter **[VBK, SAO]**

B. SPECIFIC AIM 1: SUPPORTING DATA

For assessment of degenerative changes to joint tissues, post-operative (post-op) and 18-month follow-up MRI scans will be evaluated. MRI images are obtained using a using a double-echo steady state sequence (DESS). The outer margins of the patella and femoral bone cortices, as well as the surface of the articular cartilage, are outlined from the DESS MR images using solid-modeling software (Rhinoceros, Robert NcNeel and Associates, Seattle, WA)[4,5]. Next, each outline is placed in the appropriate spatial plane so that the curves can be compiled to generate 3D surface models of the patella and femur, and respective articular cartilage (Geomagic Studio, Research Triangle Park, NC). Changes in cartilage thickness between post-operative and 18-month follow-up images will be quantified.

The effect of metal hardware used to fix the articular fracture is evident in the scan and obscures the tibial plateau articular surface (**Figure B1**, black shadow). However, the articular cartilage in the patella and femoral condyle is clearly visible at the patella-femoral joint. The articular cartilage surface of the patella is outlined in green on sagittal images from both the post-op and 18-month MRI scans in **Figure B1**. Thickness maps of the patella cartilage demonstrate regions of cartilage thinning at 18 months compared to post-operative scans (**Figure B2**). Changes in cartilage thickness will be quantified by creating a grid of sampling points spanning the articular surface of each joint.

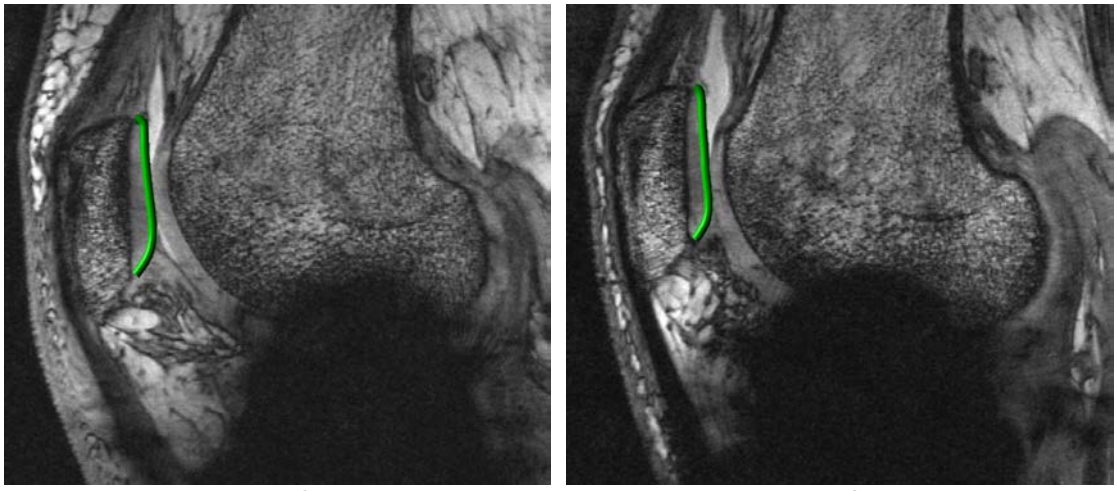

Post-Operative MRI 18-Month MRI

Figure B1. Sagittal view of PTA002 MRI scans. Green outline indicates articular cartilage surface of the patella in both images.

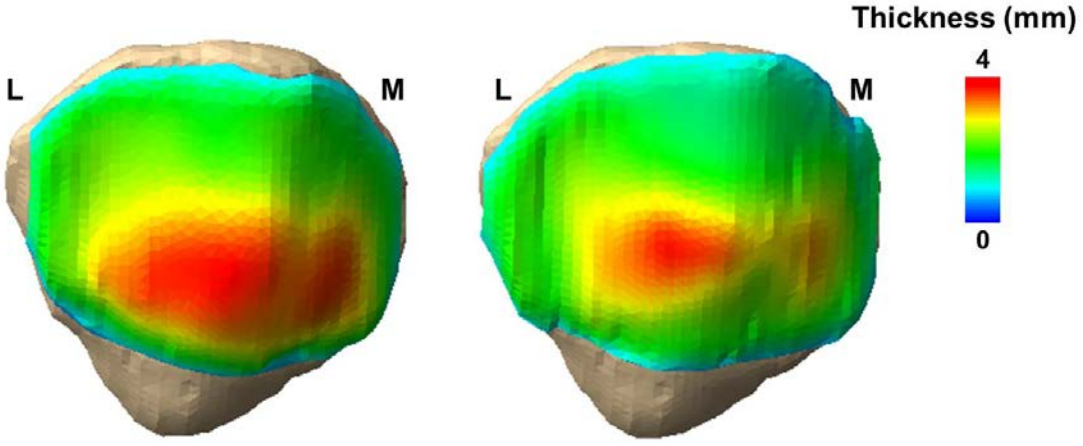

Post-Operative MRI 18-Month MRI

Figure B2. Patella cartilage thickness map of post-operative and 18-month follow-up MRI scans for subject PTA002.

Multiplex ELISA assays were used to quantify acute inflammatory and injury markers (40 analytes) in serum and synovial fluid and a summary of the data is presented in Table 1. Additional assays completed to quantify inflammatory and injury markers of joint degradation (matrix metalloproteinase (MMP)-1, -2, -3, -9, -10, and cartilage oligomeric matrix protein (COMP) in serum and synovial fluid, sulfated glycosaminoglycans (sGAG) in synovial fluid and C-terminal telopeptide of type II collagen (CTXII) in synovial fluid and urine) as well as markers of bone metabolism (C-terminal telopeptide of type I collagen (CTXI), osteocalcin, osteopontin, and osteonectin) in serum. The mean concentrations of these analytes are presented in Table 2.

Additionally, a targeted proteomics panel (designed by the Kraus laboratory to identify knee osteoarthritis progressors) is being used to assess serum in this cohort. The targeted panel will quantify 20 analytes in sera via mass spectrometry based multiple reaction monitoring (MRM). MRM analysis has been completed, and we are awaiting results of statistical analysis.

C. SPECIFIC AIM 2: TASKS

Task 1. Review and approval of animal protocol (months 1-4) **[FG] COMPLETED**

- Duke IACUC application submitted on 07/02/2012
- Duke IACUC application approved on 07/25/2012
- Duke certification of IACUC Review and Approval/Grant concordance received on 08/21/2012
- Amendment to Duke IACUC to allow use of live microCT scanning submitted 06/10/2013.
- Amendment to Duke IACUC to allow use of live microCT scanning approved 07/17/2013.

Task 2. USAMRMC Office of Research Protections review and approval of animal use documents (months 1-4) **[FG] COMPLETED**

- ACURO animal use appendix submitted to USAMRMC Office of Research Protections for review on 08/29/2012
- Received ACURO approval letter on 11/29/2012
- Amendment to allow use of live microCT scanning submitted to ACURO 08/12/2013.
- Amendment to allow use of live microCT scanning approved to ACURO 08/20/2013.

Task 3. Obtain mice and create closed intra-articular fracture of the left knee of mice (months 5-9) **[FG] COMPLETED**

3a. Obtain C57BL/6 and MRL/MpJ mice at 8 weeks of age

- 60 mice were ordered on 01/07/2013 **[FG]**
  - 30 C57BL/6 mice were received at 9 weeks of age on 01/16/2013 **[FG]**
  - 30 MRL/MpJ mice were received at 10 weeks of age on 01/24/2013 **[FG]**
- Replacement C57BL/6 mice were ordered after receiving credit for 12 mice on 05/13/2013 **[FG]**
  - 12 C57BL/6 mice were received at 10 weeks of age on 05/22/2013 **[FG]**
  - 2 C57BL/6 mice died due to unidentified health reasons on 05/26/2013 **[FG]**
  - 2 replacement C57BL/6 mice were received after credit on 08/07/2013 **[FG]**

3b. Allow mice to mature to 16 weeks of age

- Mice (30 MRL/MpJ and 18 C57BL/6) were housed until 03/04/2013 **[FG]**
- 10 C57BL/6 mice were housed until 07/17/2013 **[FG]**

3c. Create closed intra-articular fractures in the left knee of mice

- Fractures were created 03/05/2013 – 03/13/2013 **[FG]**

- Fractures (n=6) were created on 07/17/2013 **[FG]**

Task 4. Sacrifice mice and harvest samples for analyses (months 10-11) **[FG] COMPLETED**

4a. Sacrifice mice at pre-fracture, 0, 1, 7 and 14 days
4b. Collect serum and synovial fluid at time of sacrifice and store at -80°
4c. Harvest both hind limbs for analyses, store at -20°

- Mice were sacrificed (MRL/MpJ at pre-fracture, 0, 1, 7 and 14 days post-fracture and C57BL/6 at 0,1, and 7 days post-fracture) on 03/04/2013 – 03/27/2013 **[FG]**
  - Serum and synovial fluid were collected at time of sacrifice and stored at -80° **[FG, VBK]**
  - Both hind limbs were harvested at time of sacrifice and stored at -20° **[FG, VBK]**
- Mice were sacrificed (C57BL/6 at pre-fracture & 14 days post-fracture) on 07/31/2013 **[FG]**
  - Serum and synovial fluid were collected at time of sacrifice and stored at -80° **[FG, VBK]**
  - Both hind limbs were harvested at time of sacrifice and stored at -20° **[FG, VBK]**
- Mice were sacrificed (C57BL/6 at pre-fracture) on 08/08/2013. **[FG]**
  - Serum and synovial fluid were collected at time of sacrifice and stored at -80° **[FG, VBK]**
  - Both hind limbs were harvested at time of sacrifice and stored at -20° **[FG, VBK]**

Task 5. Perform microCT analyses on hind limbs (months 12-18) **[FG] COMPLETED**

- Limbs were scanned 09/04/2013-09/09/2013 **[FG]**
- Data processing and analysis complete for both hind legs **[FG]**

Task 6. Perform histologic analyses on hind limbs (months 18-24) **[FG] COMPLETED**

- Limbs were decalcified, dehydrated, and embedded in paraffin for histology **[FG]**
- Histologic grading and statistical analysis complete for both hind legs **[FG]**

Task 7. Obtain 24 additional mice and create closed intra-articular fracture of the left knee of mice (month 12-16) **[FG] COMPLETED**

7a. Obtain 12 C57BL/6 mice and 12 MRL/MpJ mice at 8 weeks of age

- 24 mice were ordered on 07/29/2013 **[FG]**
  - 12 C57BL/6 mice were received at 9 weeks of age on 08/07/2013
  - 12 MRL/MpJ mice were received at 8 weeks of age on 08/15/2013
  - 2 C57BL/6 mice died due to unidentified health reasons on 08/13/2013 **[FG]**
  - 2 replacement C57BL/6 mice were received after credit on 08/28/2013 **[FG]**

7b. Allow mice to mature to 16 weeks of age **[FG]**
7c. Create closed intra-articular fractures in the left knee of mice **[FG]**

Task 8. Sacrifice mice and harvest samples for analyses (months 17-18) **[FG, VBK] COMPLETED**

8a. C57BL/6 mice and MRL/MpJ mice were sacrificed at 56 days post-fracture **[FG]**
8b. Collected serum and synovial fluid at time of sacrifice and stored at -80° **[FG, VBK]**
8c. Both hind limbs were harvested and stored at -20° **[FG]**

Task 9. Perform microCT analyses on hind limbs (months 19-24) **[FG] COMPLETED**

- Limbs were scanned ex-vivo **[FG]**
- Data processing and analyses complete for both hind legs **[FG]**

Task 10. Perform histologic analyses on hind limbs (months 25-32) **[FG]**

- Samples processed, section and stained **[FG]**

- Additional histology grading and analyses to be completed during next quarter **[FG]**

Task 11. Determine biomarkers from Aim 1 that should be added to mouse biomarker analysis (months 30-32) **[SAO, FG, VBK]**

- Delayed due to slow enrollment of patients in Aim 1

Task 12. Perform assays to assess levels of markers (months 32-36) **[VBK]**

- Concentrations of bone biomarkers were quantified in longitudinal serum collected from second group of C57BL/6 and MRL/MpJ mice **[VBK]**
- Selection of additional assays delayed due to slow enrollment of patients in Aim 1

D. SPECIFIC AIM 2: SUPPORTING DATA

Bone Morphological Changes Correlate with Reduction in PTA after Articular Fracture in the MRL/MpJ Mouse

The objective was to identify differences in acute joint pathology and degeneration in the articular cartilage as well as other joint tissues, including the synovium and periarticular bone following articular fracture in C57BL/6 and MRL/MpJ mice.

Six mice from each strain (C57BL/6 and MRL/MpJ) did not receive a fracture and served as pre-fracture controls. Mice were sacrificed at 0, 1, 7, 14, and 56 days after fracture (n=6-11 per strain per time point). The left (fractured) and right (non-fractured) limbs were harvested, formalin fixed and scanned with microCT to assess bone morphology in the tibial epiphysis and metaphysis and femoral condyles. Histology sections (FFPE, 8μm thick in coronal plane) of all limbs were assessed for cartilage degeneration in the lateral and medial femoral condyles (LF, MF) and lateral and medial aspects of the tibial plateau (LT, MT) using a modified Mankin score, synovial inflammation using a modified synovitis score with semi-quantitative scales, and osteophyte score. Parametric analyses were performed for bone morphological measures and histological assessment.

Mankin scores of cartilage degeneration (**Figure D1**) were significantly greater in the C57BL/6 strain compared to the MRL/MpJ strain in both the lateral femur ($p=0.0204$) and the medial tibia ($p=0.0015$). Subchondral bone thickening was significantly increased in the C57BL/6 mice compared to the MRL/MpJ mice in the medial femur ($p=0.03$) and the medial tibia ($p=0.01$), but not on the lateral side. Bone morphological changes in response to fracture were significantly different between the two mouse strains. In the fractured limbs, bone mineral density (BMD), bone volume (BV), and bone fraction (BV/TV) in both the tibial epiphysis and metaphysis were significantly greater ($p<0.002$) in the MRL/MpJ strain compared to the C57BL/6 strain ($p<0.001$). However, in the femoral condyles, both BMD and cancellous bone fraction (BV/TV) were significantly increased in the C57BL/6 strain compared to the MRL/MpJ strain ($p=0.0001$).

Correlations of the histological parameters with the bone morphological parameters (**Figure D2**) showed that in tibial metaphyseal region, the Mankin total joint score negatively correlated with both the BMD ($r_s=-0.453$, $p=0.03$) and BV/TV ($r_s=-0.437$, $p=0.04$) in the MRL/MpJ strain, but did not correlate with any bone parameters in the C57BL/6 strain. The synovitis total joint score in the fractured limb positively correlated with both the BMD ($r_s=0.658$, $p=0.0001$) and BV/TV ($r_s=0.662$, $p=0.0001$) in the C57BL/6 strain, but not in the MRL/MpJ strain.

DISCUSSION: The inflammation profiles of these two mice strains differ greatly, which may account for the difference in healing after articular fracture. MRL/MpJ mice are reported to have increased levels of TGF-β_1, which may contribute to the enhanced bone response following

fracture found in this study. Interestingly, synovitis in the C57BL/6 mice was associated with greater bone changes. Previous reports have shown that C57BL/6 mice have elevated levels of pro-inflammatory cytokines IL-1 and TNF-α following joint injury. An increased local inflammatory environment may contribute to altered bone morphology and subsequent degenerative changes in the joint tissues. The difference in these arthritic profiles indicates that there may be a benefit to focusing first on fracture healing, then following up with suppression of the pro-inflammatory environment that leads to subsequent degradation of the joint. Targeted treatment needs to look at all of the joint tissues instead of focusing on a single tissue

SIGNIFICANCE: By characterizing degenerative changes in the C57BL/6 and MRL/MpJ strains, key factors that contribute to the development of PTA can be identified. By understanding what drives disease progression, potential screening methods may be developed to identify patients at high risk of developing PTA.

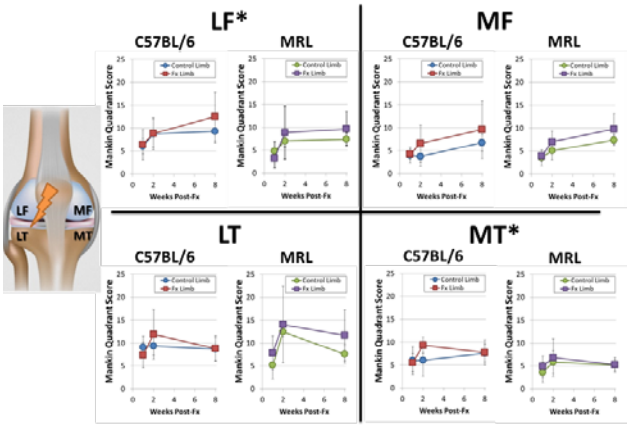

Figure D1. Cartilage degeneration assessment using a modified Mankin joint score for each quadrant shown for 7, 14, and 56 days post-fracture. Quadrants include the lateral femoral condyle (LF), lateral tibial plateau (LT), medial femoral condyle (MF), and medial tibial plateau (MT). Mean and standard deviation reported (n=6-11 per strain per time point). *denotes significance between strains by a repeated measures ANOVA (p=0.0204 in LF; p=0.0015 in MT).

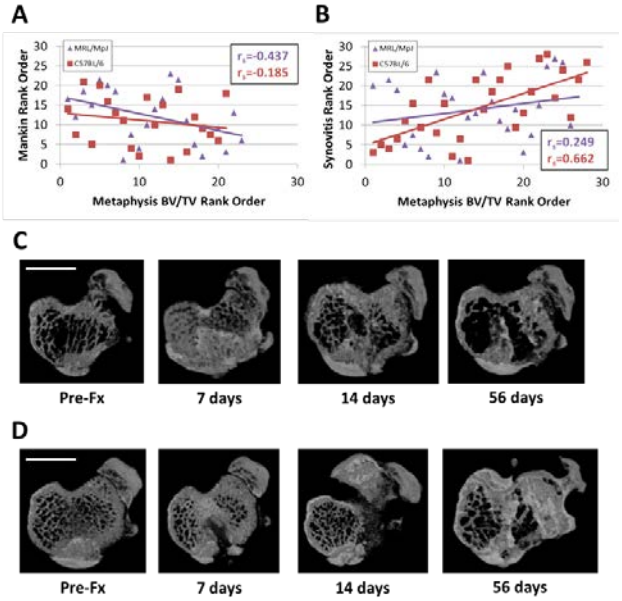

Figure D2. Correlations between Mankin total joint score, synovitis total joint score, and bone fraction (BV/TV) of the tibial metaphysis for both the MRL/MpJ and C57BL/6 strains (rank order within strain for each outcome measure, n=21-28 per strain) with Spearman correlation (R_s). **(A)** Mankin correlated with BV/TV (r_s=-0.437, p=0.0370) in MRL/MpJ strain only. **(B)** Synovitis correlated with BV/TV (r_s=0.662, p=0.0001) in C57BL/6 strain only. **(C-D)** Representative images of tibial metaphysis for **(C)** C57BL/6 strain and **(D)** MRL/MpJ strain at each time point. Scale bar is 0.5mm.

Novel *In Vivo* Micro-Computed Tomography Metrics of Joint Incongruity in the Mouse Knee Fracture Model

In vivo micro-CT scanning (SkyScan 1176, Bruker) of fractured limbs was performed before and after fracture, and then at 1, 4, and 8 weeks post-fracture. Bone surface deviations (BSD) were measured for all post-fx micro-CT scans. First, surface-rendered 3D digital models of the tibial plateau were generated from *in vivo* scans (CT-Analyser, Bruker). Models were then aligned to their respective pre-fx model's intact medial tibial plateau using an iterative closest point algorithm (Geomagic Studio, Geomagic®). BSDs were measured separately for the medial and lateral sides of the tibial plateau along three anatomic axes: antero-posterior (AP), latero-medial (LM), and axial (Geomagic Control, Geomagic®). Positive and negative deviations of the bone surface were measured, and defined as the distance to a test surface (post-fx bone surface) that was either outside (positive) or inside (negative) of the reference surface (pre-fx bone surface). A deviation of 0% corresponded to perfect alignment of pre-fx and post-fx tibial plateaus. Color maps of BSDs were generated for each anatomical direction. An example of

axial deviations in an MRL/MpJ mouse from post-fx to 8 weeks is shown in **Figure D3**. Blood was collected pre-fracture, post-fracture on day 4, and every 2 weeks to 6 weeks post-fracture. Serum concentrations of biomarkers of bone metabolism were measured, including procollagen type I N-propeptide (PINP), a bone formation marker and C-terminal telopeptide of type I collagen (CTXI), a bone resorption marker.

Temporal patterns in BSDs were significantly different between C57BL/6 and MRL/MpJ mice over 8 weeks (**Figure D3**). Significant differences were observed in the lateral tibial plateau as measured by average positive axial deviation ($p = 0.01$), average positive LM deviation ($p = 0.015$), and maximum positive LM deviation ($p = 0.01$). Additionally, a significantly larger average positive axial deviation was observed in C57BL/6 mice at 8 weeks post-fx ($p=0.01$) (**Figure D4**). In the medial plateau, significant differences were seen between strains as measured by average positive axial deviation ($p=0.049$) and average negative LM deviation ($p=0.049$). Concentrations of PINP in the C57BL/6 mice were significantly lower than the MRL/MpJ mice post-fx ($p=0.005$; **Figure D5**), indicating a less robust acute bone anabolic response compared with the superhealer strain. Despite higher levels of CTXI in the C57BL/6 mice compared to the MRL/MpJ at pre-fx, no differences were found in CTXI levels post-fx between strains or at any time point.

DISCUSSION: Through the development of novel *in vivo* micro-CT metrics of joint incongruity, we analyzed temporal patterns in bone surface deviations that revealed significant differences between C57BL/6 and MRL/MpJ strains over 8 weeks. Acute displacements of the bone surface following articular fracture were predictive of arthritis development in the C57BL/6 but not MRL/MpJ mice. Interestingly, after 8 weeks of fracture healing, we observed significantly larger bone surface deviations in C57BL/6 mice compared to MRL/MpJ mice. Additionally, C57BL/6 mice showed an acute drop in serum PINP following articular fracture compared to MRL/MpJ mice. These results indicate a less robust acute bone anabolic response compared with MRL/MpJ superhealer strain. Previous studies reported that C57BL/6 mice exhibit higher levels of inflammation post-fracture than the MRL/MpJ mice and suggested that this may contribute to the development and progression of PTA in this model. This inflammatory environment may influence fracture healing immediately post-fx, potentially predisposing C57BL/6 mice to PTA. These findings suggest that joint incongruities secondary to articular fracture alone do not predispose mice to the development of PTA, but rather differences in bone metabolism may play a role in early healing, which may have a greater effect on outcome. Our results may provide insights into the physiologic processes determining PTA outcomes that may protect the MRL/MpJ strain from the effects of articular incongruity.

SIGNIFICANCE: Our results provide evidence that the MRL/MpJ superhealer strain is able to overcome the effects of articular incongruity. More work is needed to translate the MRL/MpJ healing response into clinical therapies. *In vivo* micro-CT metrics of joint incongruity provide a method for quantifying bone surface incongruities that have traditionally been difficult to measure and provide new possibilities to guide PTA research and improve fracture management. The translational potential of our joint incongruity metrics is high, as this methodology could be applied to full scale clinical CT scans.

FIGURES

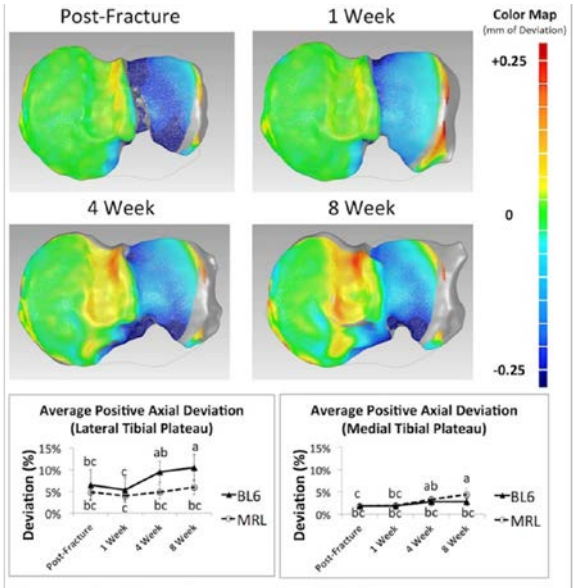

Figure D3. (Top) Representative color map of axial deviation with fracture healing. (Bottom) Significant strain-wise differences in fracture healing to 8 weeks post-fracture *(data with different letters are significantly different)*.

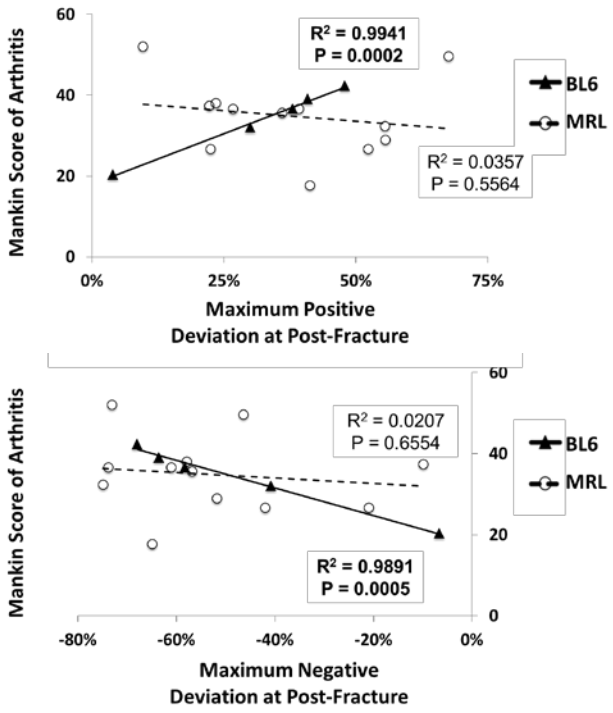

Figure D4. Correlations between total joint Mankin score for arthritis at 8 weeks post-fracture and post-fracture joint incongruity for C57BL/6 (BL6) and MRL/MpJ (MRL) mice.

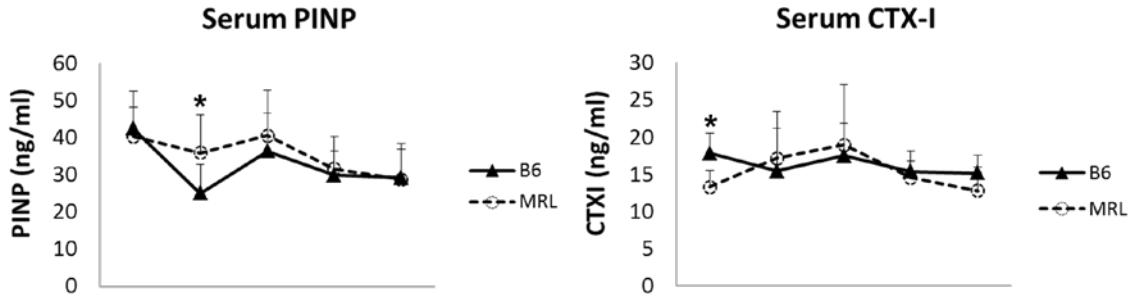

Figure D5. Serum concentrations of bone biomarkers PINP and CTX-I with articular fracture in C57BL/6 (B6) and MRL/MpJ (MRL) mice.

E. PROBLEM AREAS

Specific Aim 1:

The overall objective of this study is to identify biomarkers following articular fracture that may be predictive of the development of PTA. Specifically, patients with a closed unilateral articular fracture of the knee requiring operative treatment will be enrolled over an 18-month period. Biosamples (synovial fluid from the injured and contralateral uninjured knee, serum, and urine) will be collected prior to or at surgical intervention. MR imaging of the injured knee will be obtained to assess the articular cartilage. Degenerative changes in the cartilage and joint space narrowing will be correlated to biomarkers that may be indicative and predictive of joint degeneration and the development of PTA. After expanding the enrollment criteria and

extending the enrollment period, enrollment has closed with 20 patients successfully enrolled in the study.

Issues:
As previously reported, enrollment was initially slow. However, in response, we expanded the enrollment criteria and extended the enrollment period. The enrollment has closed with 20 patients successfully enrolled in the study. Biosamples from all enrolled patients have been collected, processed and stored at -80°C. Questionnaires have also been collected from all patients. However, there have been issues with patient compliance in obtaining MRI scans, due to various factors including claustrophobia, definitive treatment outside the study criteria, such as conversion to total knee arthroplasty or only open reduction internal fixation, and noncompliance. We have obtained post-op MRI scans for all patients still enrolled in the study. For 18-month follow-up MRI scans, we have obtained 5 scans, 1 scan is schedule for November 19, 2015, and 3 additional scans will be scheduled in December 2015. Within the next reporting period, MRI scans will continue to be analyzed **(Figures B1-B2)**. Proteomic analyses are being performed on biosamples using a targeted proteomics panel (designed by the Kraus laboratory to identify knee osteoarthritis progressors) and discovery metabolomics will be run on additional samples. Biomarker assays are being run on all collected biosamples (sera, urine and synovial fluid). These results will be compared to those obtained from the animal study in Specific Aim 2. However, due to the slow initial enrollment, we have received a one year no cost extension in order to complete all analyses.

Specific Aim 2: No problems/issues to report.

F. ANIMAL USAGE STATISTICS

- DOD Annual Report on Animal Use:
  - Species used: mice
  - Number of each species used: 84
- USDA Pain Category for all animals used:
  - Category C (Non-Painful Procedures): 12
  - Category D (Procedures using anesthesia/analgesia): 72

4. KEY ACCOMPLISHMENTS:

- Twenty total patients have been enrolled in Aim 1. With 4 disqualified and 2 dropouts, the total is fourteen, which is the target number of patients for statistical significance.
- For aim 1, we are continuing to collect, review and analyze post-op and 18 month follow-up MRI scans from enrolled patients.
- The quantification of inflammatory and injury markers, as well as markers of joint degradation and bone metabolism have been performed on serum, synovial fluid and urine biosamples.
- Targeted proteomics panel designed by the Kraus laboratory to identify knee osteoarthritis progressors has been completed on serum samples and statistical analysis is ongoing.
- All animals for Aim 2 were obtained and closed articular fractures of the tibial plateau were successfully created with a 100% success rate. Sacrifice and sample collection are complete.
- In vivo and ex vivo microCT analyses for Aim 2 are complete.
- Histologic analyses for Aim 2 are complete.

5. CONCLUSIONS:

Post-traumatic arthritis (PTA) is a severe burden in active duty and discharged soldiers. Recent figures from Operation Iraqi Freedom and Operation Enduring Freedom indicated joint

degeneration following injury is the most common cause of a soldier being unfit for duty.[3] Compared to other forms of arthritis, (PTA) has a more rapid clinical onset.[6] This rapid onset of degenerative arthritis is occurring following joint injuries in a younger population of soldiers. The goal of this work is to identify biomarkers following articular fracture that may be predictive of the development of PTA. This knowledge is needed for future investigations to assess acute interventions to prevent PTA that can be given on the battlefield or at the time of stabilizing medical care in down range medical facilities. To reach this goal, the proposed investigation studies patients who have sustained a closed, displaced articular fracture about the knee requiring operative treatment. While these patients are not suffering battlefield injuries, they do represent significant articular injuries that are at risk for developing PTA. A companion murine bench top series of experiments will allow for the comparison of human and mouse response following joint fracture. An animal model is needed to allow for a low-cost model for the assessment of future therapies to prevent PTA.

6. PUBLICATIONS, ABSTRACTS, AND PRESENTATIONS:

To date, findings from this study have been presented with abstracts at the following meetings:

a. "Novel In Vivo micro-Computed Tomography Metrics of Joint Incongruity Predict Arthritis in a Knee Fracture Model" presented in podium and poster format at the Extremity War Injuries X symposium on January 26-28, 2015.[7]

b. "Novel In Vivo micro-Computed Tomography Metrics of Joint Incongruity Predict Arthritis in a Knee Fracture Model" presented in podium format at the 2015 Annual Meeting of the Orthopaedic Research Society on March 28 -31, 2015.[8]

c. "Bone Morphological Changes Correlate with Reduction in PTA after Articular Fracture in the MRL/MpJ Mouse" presented in poster format at the 2015 Annual Meeting of the Orthopaedic Research Society on March 28 -31, 2015.[9]

d. "Joint Incongruity and Biomarkers of Bone Metabolism as Predictors of Post-traumatic Arthritis in Mice" presented in poster format at the 2015 World Congress on Osteoarthritis on April 30 - May 3, 2015.[10]

7. INVENTIONS, PATENTS AND LICENSES: Nothing to report.

8. REPORTABLE OUTCOMES: The existing measures for clinical outcome are being applied in a novel manner to articular fractures. Data points such as VAS pain scores, KOOS, and SF-36 have been completed by enrolled patients. The research is still in progress so reportable outcomes from the study are still pending.

9. OTHER ACHIEVEMENTS: None to report.

10. REFERENCES:

1. Promotion NCfCDPaH. Arthritis Meeting the Challenge At A Glance 2011. 2011. http://www.cdc.gov/chronicdisease/resources/publications/aag/arthritis.htm#chart1.

2. Brown TD, Johnston RC, Saltzman CL, Marsh JL, Buckwalter JA. Nov-Dec 2006. Posttraumatic osteoarthritis: a first estimate of incidence, prevalence, and burden of disease. J Orthop Trauma. 20(10):739-744.

3. Cross JD, Ficke JR, Hsu JR, Masini BD, Wenke JC. 2011. Battlefield orthopaedic injuries cause the majority of long-term disabilities. The Journal of the American Academy of Orthopaedic Surgeons. 19 Suppl 1:S1-7.

4. Widmyer MR, Utturkar GM, Leddy HA, et al. Oct 2013. High body mass index is associated with increased diurnal strains in the articular cartilage of the knee. Arthritis Rheum. 65(10):2615-2622.

5. Coleman JL, Widmyer MR, Leddy HA, et al. Feb 1 2013. Diurnal variations in articular cartilage thickness and strain in the human knee. J Biomech. 46(3):541-547.
6. Furman BD, Olson SA, Guilak F. Nov-Dec 2006. The development of posttraumatic arthritis after articular fracture. Journal of orthopaedic trauma. 20(10):719-725.
7. Vovos TJ, Furman BD, Kimmerling KA, et al. Novel in vivo micro-computed tomography metrics of joint incongruity predict arthritis in a knee fracture model. Paper presented at: Extemity War Injuries X: Return to Health and Function; January 26-28, 2015, 2015; Washington, DC.
8. Vovos TJ, Furman BD, Kimmerling KA, et al. Novel in vivo microCT metrics of joint incongruity predict arthritis in a knee fracture model. Paper presented at: Annual Meeting of the Orthopaedic Research Society2015; Las Vegas, NV.
9. Kimmerling KA, Furman BD, Vovos TJ, Huebner JL, Guilak F, Olson SA. Bone Morphological Changes Correlate with Reduction in PTA after Articular Fracture in the MRL/MpJ Mouse. Paper presented at: Annual Meeting of the Orthopaedic Research Society2015; Las Vegas, NV.
10. Vovos TJ, Furman BD, Huebner JL, et al. 2015. Joint incongruity and biomarkers of bone metabolism as predictors of post-traumatic arthritis in mice. Osteoarthritis and Cartilage. 23:A242-A243.

11. APPENDICES:

Abstracts are included from the 2015 Extremity War Injuries X symposium, 2015 Annual Meeting of the Orthopaedic Research Society and 2015 World Congress on Osteoarthritis in which findings from this study were presented.

Table 1. Biomarker Concentrations from MSD Human 40-plex ELISA (Mean (SD))

	Synovial Fluid				Serum	
	BL Fx	BL Non-Fx	V2 Fx	V2 Non-Fx	BL	V2
Pro-inflammatory Panel	n=14	n=10	n=4	n=2	n=14	n=4
IFN-γ (pg/ml)	34.72 (50.36)	2.00 (2.31)	51.65 (55.87)	1.14 (0.41)	5.34 (10.43)	4.87 (3.57)
IL-1β (pg/ml)	1.69 (1.53)	0.01 (0.03)	4.52 (2.88)	0.05 (0.07)	0.00 (0.00)	0.00 (0.00)
IL-2 (pg/ml)	1.62 (2.25)	0.32 (0.27)	5.94 (7.59)	0.42 (0.02)	0.27 (0.36)	0.23 (0.05)
IL-4 (pg/ml)	1.49 (1.30)	0.08 (0.10)	3.63 (3.42)	0.08 (0.12)	0.03 (0.02)	0.03 (0.02)
IL-6 (pg/ml)	6117.67 (8645.85)	31.89 (90.50)	6181.18 (3940.05)	2.28 (0.91)	5.69 (6.42)	5.17 (2.15)
IL-8 (pg/ml)	1195.24 (1108.07)	27.01 (43.79)	4097.79 (4783.45)	8.10 (0.54)	14.60 (10.90)	17.69 (6.12)
IL-10 (pg/ml)	5.19 (4.69)	0.20 (0.20)	4.89 (3.05)	0.11 (0.06)	0.51 (0.48)	0.34 (0.13)
IL-12p70 (pg/ml)	1.64 (1.62)	0.24 (0.13)	2.03 (2.23)	0.23 (0.03)	0.17 (0.04)	0.17 (0.05)
IL-13 (pg/ml)	9.53 (7.09)	0.94 (0.75)	22.75 (20.15)	1.06 (0.76)	1.07 (0.48)	0.98 (0.50)
TNF-α (pg/ml)	4.30 (2.23)	1.27 (0.75)	5.93 (4.19)	1.18 (0.26)	2.23 (0.65)	3.11 (0.98)
Cytokine Panel						
GM-CSF (pg/ml)	0.48 (0.33)	0.25 (0.16)	0.68 (0.57)	0.14 (0.08)	0.07 (0.09)	0.04 (0.04)
IL-1α (pg/ml)	0.42 (0.66)	0.05 (0.09)	0.27 (0.23)	0.52 (0.74)	0.07 (0.23)	0.05 (0.10)
IL-5 (pg/ml)	4.97 (14.13)	0.00 (0.00)	9.82 (15.26)	0.00 (0.00)	0.04 (0.10)	0.08 (0.15)
IL-7 (pg/ml)	2.44 (2.01)	5.76 (4.81)	6.88 (10.40)	3.89 (0.01)	22.20 (12.27)	25.68 (13.73)
IL-12/IL-23p40 (pg/ml)	150.57 (144.01)	47.84 (48.62)	245.11 (337.19)	20.08 (7.32)	85.93 (51.86)	152.66 (131.22)
IL-15 (pg/ml)	11.28 (6.66)	9.17 (4.82)	14.52 (4.40)	11.38 (3.31)	2.78 (2.32)	3.48 (2.56)
IL-16 (pg/ml)	1142.07 (975.60)	342.82 (272.35)	891.53 (431.19)	161.52 (69.16)	235.64 (337.42)	191.38 (93.94)
IL-17A (pg/ml)	7.24 (14.94)	1.37 (1.62)	17.29 (15.69)	0.40 (0.12)	2.35 (1.22)	3.50 (1.85)
TNF-β (pg/ml)	0.26 (0.15)	0.13 (0.07)	0.39 (0.20)	0.10 (0.01)	0.14 (0.14)	0.41 (0.47)
VEGF (pg/ml)	1843.56 (1114.17)	246.84 (199.76)	2775.26 (1658.43)	210.65 (182.61)	107.28 (51.66)	257.91 (188.76)
Chemokine Panel						
Eotaxin (pg/ml)	48.79 (32.11)	19.45 (20.79)	60.67 (28.50)	18.83 (0.66)	63.92 (39.33)	81.68 (49.60)
Eotaxin-3 (pg/ml)	51.91 (43.02)	4.41 (4.60)	93.10 (97.80)	0.67 (0.94)	8.98 (7.62)	16.74 (7.44)
IP-10 (pg/ml)	1193.82 (980.23)	396.82 (561.40)	3819.12 (3886.94)	162.82 (39.67)	188.52 (94.92)	306.78 (176.76)
MIP-1α (pg/ml)	46.01 (52.26)	202.21 (532.90)	53.96 (52.77)	8.89 (0.82)	216.17 (615.20)	337.48 (652.04)
MIP-1β (pg/ml)	100.97 (66.69)	43.30 (27.96)	50.01 (18.80)	24.47 (0.05)	107.83 (100.17)	97.81 (15.45)
MCP-1 (pg/ml)	1719.75 (1147.57)	233.03 (125.03)	1972.54 (1115.86)	184.94 (20.37)	248.85 (116.83)	222.42 (42.81)
MCP-4 (pg/ml)	78.74 (91.26)	34.66 (26.72)	129.26 (113.48)	16.27 (6.46)	137.36 (93.32)	131.63 (43.03)
MDC (pg/ml)	4063.12 (6146.94)	416.23 (206.33)	15373.97 (24122.25)	287.58 (266.97)	1378.39 (719.91)	1341.88 (679.37)
TARC (pg/ml)	86.64 (58.51)	43.80 (49.40)	99.80 (80.05)	19.10 (17.03)	312.70 (258.51)	301.32 (157.24)
Angiogenesis Panel						
bFGF (pg/ml)	93.31 (149.14)	158.63 (364.24)	16.94 (20.01)	28.51 (27.26)	25.10 (20.94)	17.22 (17.56)
Flt-1 (pg/ml)	2356.42 (1391.84)	213.47 (145.84)	2833.83 (1565.26)	293.93 (194.97)	102.44 (27.68)	131.09 (79.46)
PIGF (pg/ml)	3385.15 (2169.18)	333.66 (681.58)	3488.53 (1847.78)	169.19 (132.20)	27.65 (9.57)	36.67 (4.85)
Tie-2 (pg/ml)	2719.72 (1115.85)	1319.02 (1539.96)	1959.23 (930.10)	510.22 (294.36)	3788.92 (829.95)	3325.44 (672.95)
VEGF (pg/ml)	9444.28 (4255.23)	975.52 (751.83)	9678.99 (3636.31)	1002.21 (1072.74)	477.39 (209.18)	1093.72 (838.91)
VEGF-C (pg/ml)	675.60 (477.56)	115.27 (109.65)	1042.55 (701.10)	64.18 (72.20)	412.53 (125.02)	360.38 (71.31)
VEGF-D (pg/ml)	840.49 (440.20)	306.27 (231.94)	1005.24 (585.59)	426.05 (133.22)	593.07 (228.89)	700.39 (308.86)
Vascular Injury						
CRP (ng/ml)	8936.33 (8217.06)	3624.04 (2664.70)	49593.27 (32925.18)	8516.75 (5800.99)	34858.84 (47077.89)	96916.98 (48965.4)
SAA (ng/ml)	25100.46 (46440.13)	6195.64 (12390.13)	34131.26 (30008.93)	6305.41 (1541.06)	79290.91 (91067.18)	178943.8 (70304.67)
VCAM-1 (ng/ml)	416.61 (239.05)	194.95 (166.68)	459.86 (309.16)	81.48 (46.30)	422.94 (148.31)	547.21 (213.16)
ICAM-1 (ng/ml)	621.92 (274.68)	301.72 (211.34)	941.65 (322.31)	227.53 (135.92)	545.54 (108.91)	679.53 (118.88)

BL= baseline; V2= visit 2; Fx = fracture

Table 2. Concentrations of Biomarkers of Joint and Bone Metabolism (Mean (SD))

	Synovial Fluid				Serum	
	BL Fx	BL Non-Fx	V2 Fx	V2 Non-Fx	BL	V2
Joint Metabolism	n=14	n=10	n=4	n=2	n=14	n=4
MMP-1 (pg/ml)	2650446 (3484142)	81185.55 (227578.2)	4106354 (3255922)	2735.29 (1784.85)	23043.6 (19380.81)	22139.71 (12344.98)
MMP-2 (pg/ml)	129558.3 (53484.38)	90483.43 (21840.06)	171377.9 (31439.92)	115022.4 (1936.80)	56586.26 (11680.12)	60596.31 (14943.09)
MMP-3 (pg/ml)	3868196 (3664329)	1278008 (3547357)	4859359 (3199642)	305677.6 (197044.3)	21371.47 (22112.01)	44594.18 (63215.51)
MMP-9 (pg/ml)	58854.76 (92035.04)	42747.11 (87430.98)	53408.05 (46548.22)	4011.69 (2210.20)	197221.4 (151946.3)	256615.8 (152129)
MMP-10 (pg/ml)	1530.1 (1209.31)	537.69 (323.61)	1899.10 (858.83)	536.21 (84.55)	794.2669 (405.47)	948.93 (462.95)
COMP (ng/ml)	33995.18 (19554.78)	36262.78 (20055.86)	42609.63 (13439.4)	30879.25 (4180.77)	348.28 (206.47)	284.875 (166.17)
***CTXII (ng/ml)**	0.35 (0.15)	0.38 (0.15)	0.46 (0.31)	0.46 (0.05)	-	-
sGAG (pg/ml)	275.46 (249.82)	116.04 (55.83)	403.77 (196.25)	172.69 (155.31)	-	-
HA (ng/ml)					38.13 (38.29)	43.94 (13.82)
Bone Metabolism						
CTXI (ng/ml)					0.70 (0.25)	0.95 (0.31)
Osteocalcin (ng/ml)					202.80(94.57)	216.92 (102.82)
Osteopontin (ng/ml)					25.75 (13.79)	39.80 (10.16)
Osteonectin (ng/ml)					1632.56 (546.87)	1936.14 (765.11)

***Urinary CTXII corrected for Creatinine was measured in both BL (406.35 ng/mmolCr (305.10); n=14) and V2 (643.13 ng/mmolCr (478.86); n=4) urine samples**

BL= baseline; V2 = visit 2; Fx = fracture

APPENDICES:

We have included abstracts from the following meetings in which findings from this study were presented:

- “Novel In Vivo micro-Computed Tomography Metrics of Joint Incongruity Predict Arthritis in a Knee Fracture Model” presented in podium and poster format at the Extremity War Injuries X symposium on January 26-28, 2015
- “Bone Morphological Changes Correlate with Reduction in PTA after Articular Fracture in the MRL/MpJ Mouse” presented in poster format at the 2015 Annual Meeting of the Orthopaedic Research Society on March 28 -31, 2015.
- “Novel In Vivo micro-Computed Tomography Metrics of Joint Incongruity Predict Arthritis in a Knee Fracture Model” presented in podium format at the 2015 Annual Meeting of the Orthopaedic Research Society on March 28 -31, 2015.
- “Joint Incongruity and Biomarkers of Bone Metabolism as Predictors of Post-traumatic Arthritis in Mice” presented in poster format at the 2015 World Congress on Osteoarthritis on April 30 - May 3, 2015.

American Academy of Orthopaedic Surgeons / Orthopaedic Trauma Association
Society of Military Orthopaedic Surgeons / Orthopaedic Research Society

Extremity War Injuries X: Return to Health and Function

January 26-28, 2015 / Mandarin Oriental Hotel / Washington, DC

Symposium Co-Chairs: Marc Swiontkowski, MD and Col Jeffrey Davila, MD
EWI Project Team Chair: COL (Ret.) James Ficke, MD

POSTER SESSION CALL FOR ABSTRACTS

Deadline: December 1, 2014

The American Academy of Orthopaedic Surgeons (AAOS) is accepting abstracts for combat casualty and/or trauma related research. Up to 16 abstracts will be selected for display at the 2015 Extremity War Injuries Symposium (EWI), January 26-28, at the Mandarin Oriental Hotel in Washington, DC.

If your abstract is accepted for exhibition, your poster will be displayed January 27 and 28, with a poster session from 6:00 – 8:00 PM on Tuesday, January 27. You must be present to participate in the poster session. Selected posters will be invited to give a brief podium presentation on Wednesday, January 28. The $600 EWI registration fee will be waived for poster presenters. Presenters will be responsible for hotel and travel costs associated with attending the EWI symposium. CME (up to 14.75 hours) will be available for EWI X attendees/participants.

Please complete this form and submit with a copy of your CV to Erin Ransford, AAOS Manager, Research Advocacy, at ransford@aaos.org by Monday, December 1, 2014.

Full Name: Steven A. Olson
Military Rank (if applicable):
Institution/Organization: Duke University School of Medicine
Mailing Address: DUMC 3389
City /State/Zip: Durham, NC 27710
Email: olson016@dm.duke.edu
Phone: 919-668-3000

Abstract Title: Novel In Vivo micro-Computed Tomography Metrics of Joint Incongruity Predict Arthritis in a Knee Fracture Model

Abstract Text (limited to 3,000 characters, including spaces [~500 words])
The form will expand as you type/paste text.

Introduction: Post-traumatic arthritis (PTA) is an accelerated form of arthritis that develops following joint injury and occurs most predictably after intraarticular fracture. The MRL/MpJ strain of mice is protected from PTA following intraarticular fracture, thus providing valuable insight into the mechanisms of progression of PTA. We hypothesized that quantitative measures of joint incongruity could be used to predict PTA development following intraarticular fracture by assessing in vivo micro-CT metrics of joint incongruity after joint fracture. Furthermore, we hypothesized that the MRL/MpJ mouse would have an altered fracture healing response compared to the C57BL/6 mouse.

Methods: This is an IACUC-approved protocol. Skeletally mature male C57BL/6 (n=12, Charles River) and MRL/MpJ mice (n=12, Jackson Labs) were subjected to a closed intraarticular fracture (fx) of the lateral tibial plateau using an established model. In vivo micro-CT (SkyScan 1176, Bruker) of fractured limbs was performed pre and post fracture, and then at 1, 4, & 8 weeks post-fx. The articular surface alignment was assessed as bone surface deviations (BSD) for all post-fx micro-CT scans. Surface-rendered 3D digital models of the tibial plateau were generated from in vivo scans. Models were aligned to their respective pre-fx model's intact medial tibial plateau using an iterative closest point algorithm. BSDs were measured separately for the medial and lateral tibial plateau along three anatomic axes: anteroposterior (AP), latero-medial (LM), and axial. Positive and negative deviations of the bone surface were measured as the distance a displaced surface that was either outside (positive) or inside (negative) of the intact surface. A deviation of 0% corresponded to perfect alignment of pre-fx and post-fx tibial plateaus.

Results: Intraarticular fractures were successfully created in all mice. Temporal patterns in BSDs were significantly different between C57BL/6 and MRL/MpJ mice over 8 weeks. The initial displacement of BSD was similar in each strain and was observed to increase over time in the C57BL/6 to be significantly different from the MRL/MpJ at 8 weeks post fracture ($p=.01$).

In assessing the relationship between BSDs of the joint after fracture and the development of PTA, total joint Mankin scores of PTA changes were correlated to all BSDs measured in both mouse strains. Measures of BSDs from scans obtained immediately after fracture showed the strongest correlations with PTA development. In C57BL/6 mice, BSDs on post-fx day 0 were highly predictive of PTA severity at 8 weeks post-fx ($R^2=0.94$, $p=0.006$). In contrast, MRL/MpJ mice post-fx day 0 BSDs did not predict the development of PTA ($R^2=0.25$, $p=0.10$).

Significance: The MRL/MpJ mice are protected against development of PTA, and their post injury response overcomes the effect of articular misalignment. Whereas the C57BL/6 post injury response enhances the effect of articular misalignment.

Bone Morphological Changes Correlate with Reduction in PTA after Articular Fracture in the MRL/MpJ Mouse

Kelly A. Kimmerling, MEng[1], Bridgette D. Furman, B.S.[2], Tyler J. Vovos, BS[1], Janet L. Huebner, MS[3], Virginia B. Kraus, MD, PhD[2], Farshid Guilak, PhD[2], Steven A. Olson, MD[2].
[1]Duke University, Durham, NC, USA, [2]Duke University Medical Center, Durham, NC, USA, [3]Duke Molecular Physiology Institute, Durham, NC, USA.

Disclosures: K.A. Kimmerling: None. **B.D. Furman:** None. **T.J. Vovos:** None. **J.L. Huebner:** None. **V.B. Kraus:** 5; Bioiberica. **F. Guilak:** 3A; Cytex Therapeutics Inc.. 4; Cytex Therapeutics Inc.. 7; Elsevier Ltd. **S.A. Olson:** 3B; Bioventis. 5; Synthes USA, Bioventis.

Introduction: Post-traumatic arthritis (PTA) occurs after joint trauma, such as articular fractures, but the mechanism is not well-understood [1, 2, 3]. While PTA can occur rapidly after moderate to severe articular injuries, not every patient will go on to develop this condition. Currently, there are no effective screening methods to determine who is at risk. Characterizing degenerative changes in joint tissues following articular fracture in an animal model provides an opportunity to study the pathology of joint injury and the development of PTA. In previous studies, we have shown that C57BL/6 mice exhibit arthritic changes following articular fracture, whereas the MRL/MpJ strain is protected from PTA [1, 4]. The objective of this study was to identify differences in acute joint pathology and degeneration in C57BL/6 and MRL/MpJ mice as measured in the articular cartilage, synovium, and periarticular bone following articular fracture.

Methods: All animal procedures were performed in accordance with an IACUC-approved protocol. Male C57BL/6 and MRL/MpJ mice (n=83) were subjected to an articular fracture at 16 weeks of age using an established model [5]. Six mice from each strain did not receive a fracture and served as pre-fracture controls. Mice were sacrificed at 0, 1, 7, 14, and 56 days after fracture (n=6-11 per strain per time point). The left (fractured) and right (non-fractured) limbs were harvested, formalin fixed and scanned with microCT to assess bone morphology in the tibial epiphysis and metaphysis and femoral condyles. Histology sections (FFPE, 8µm thick in coronal plane) of all limbs were assessed for cartilage degeneration in the lateral and medial femoral condyles (LF, MF) and lateral and medial aspects of the tibial plateau (LT, MT) using a modified Mankin score, synovial inflammation using a modified synovitis score with semi-quantitative scales, and osteophyte score [1,5,6,7,8]. Parametric analyses were performed for bone morphological measures and histological assessment.

Results: Mankin scores of cartilage degeneration were significantly greater in the C57BL/6 strain compared to the MRL/MpJ strain in both the lateral femur ($p=0.0204$) and the medial tibia ($p=0.0015$). No strain differences were seen in the lateral tibia, where the fracture occurred, or in the medial femur. Synovial inflammation did not differ by strain; however, there was a significant increase in the fractured limb compared to the control limb at 1 and 2 weeks post-fracture ($p<0.05$). Osteophyte scores did not show any trends, but were present in both strains at 7 and 14 days and were not present at 56 days. Subchondral bone thickening was significantly increased in the C57BL/6 mice compared to the MRL/MpJ mice in the medial femur ($p=0.0278$) and the medial tibia ($p=0.0077$), but not on the lateral side.

Bone morphological changes in response to fracture were significantly different between the two mouse strains. In the fractured limbs, bone mineral density (BMD), bone volume (BV), and bone fraction (BV/TV) in both the tibial epiphysis and metaphysis were significantly greater ($p<0.0015$) in the MRL/MpJ strain compared to the C57BL/6 strain ($p<0.001$). However, in the femoral condyles, both BMD and cancellous bone fraction (BV/TV) were significantly increased in the C57BL/6 strain compared to the MRL/MpJ strain ($p=0.0001$).

Correlations of the histological parameters with the bone morphological parameters showed that in tibial metaphyseal region, the Mankin total joint score negatively correlated with both the BMD ($rs=-0.453$, $p=0.0298$) and BV/TV ($rs=-0.437$, $p=0.0370$) in the MRL/MpJ strain, but did not correlate with any bone parameters in the C57BL/6 strain. The synovitis total joint score in the fractured limb positively correlated with both the BMD ($rs=0.658$, $p=0.0001$) and BV/TV ($rs=0.662$, $p=0.0001$) in the C57BL/6 strain, but not in the MRL/MpJ strain.

Discussion: Analysis of both histologic and bone morphologic measures in this study suggest that the differences between the C57BL/6 and MRL/MpJ strains may be associated with bone morphological changes. Despite the lack of difference in synovial inflammation between strains, cartilage degradation and bone parameters were significantly different, which may account for the altered healing response after articular fracture [4]. MRL/MpJ mice are reported to have increased levels of TGF-β1, which may contribute to the enhanced bone response following fracture found in this study [9]. Interestingly, synovitis in the C57BL/6 mice was associated with greater bone changes. Previous reports have shown that C57BL/6 mice have elevated levels of pro-inflammatory cytokines IL-1 and TNF-α following joint injury [1]. An increased local inflammatory environment may contribute to altered bone morphology and subsequent degenerative changes in the joint tissues. The difference in these arthritic profiles indicates that there may be a benefit to focusing first on fracture healing, then following up with suppression of the pro-inflammatory environment that leads to subsequent degradation of the joint. Clinically, surgical restoration of the articular surface is the only treatment for articular fractures. To date, there is no method of identifying patients that are at risk for developing PTA. In addition to measures of joint pathology, serum and synovial fluid from both strains of mice will be analyzed for biomarkers. The comparison of early imaging or biochemical biomarkers between mice strains and humans, which are predictive of PTA, may be useful in assessing clinical risk in articular fracture patients.

Significance: By characterizing degenerative changes in the C57BL/6 and MRL/MpJ strains, key factors that contribute to the development of PTA can be identified. By understanding what drives disease progression, potential screening methods may be developed to identify patients at high risk of developing PTA.

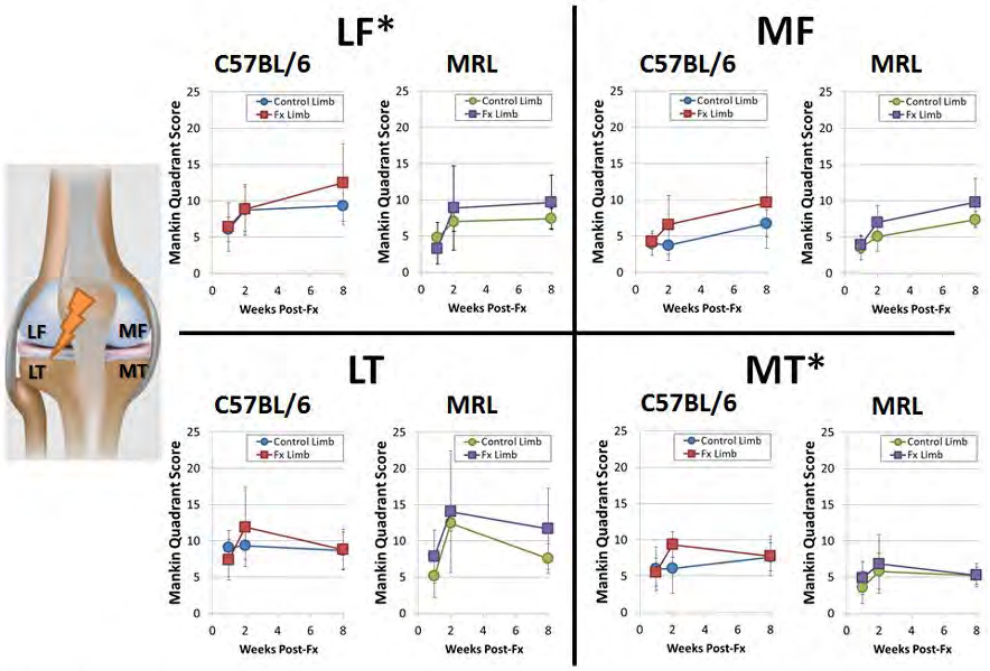

Figure 1

Cartilage degeneration assessment using a modified Mankin joint score for each quadrant shown for 7, 14, and 56 days post-fracture. Quadrants include the lateral femoral condyle (LF), lateral tibial plateau (LT), medial femoral condyle (MF), and medial tibial plateau (MT). Mean and standard deviation reported (n=6-11 per strain per time point). * denotes significance between strains by a repeated measures ANOVA ($p=0.0204$ in LF; $p=0.0015$ in MT).

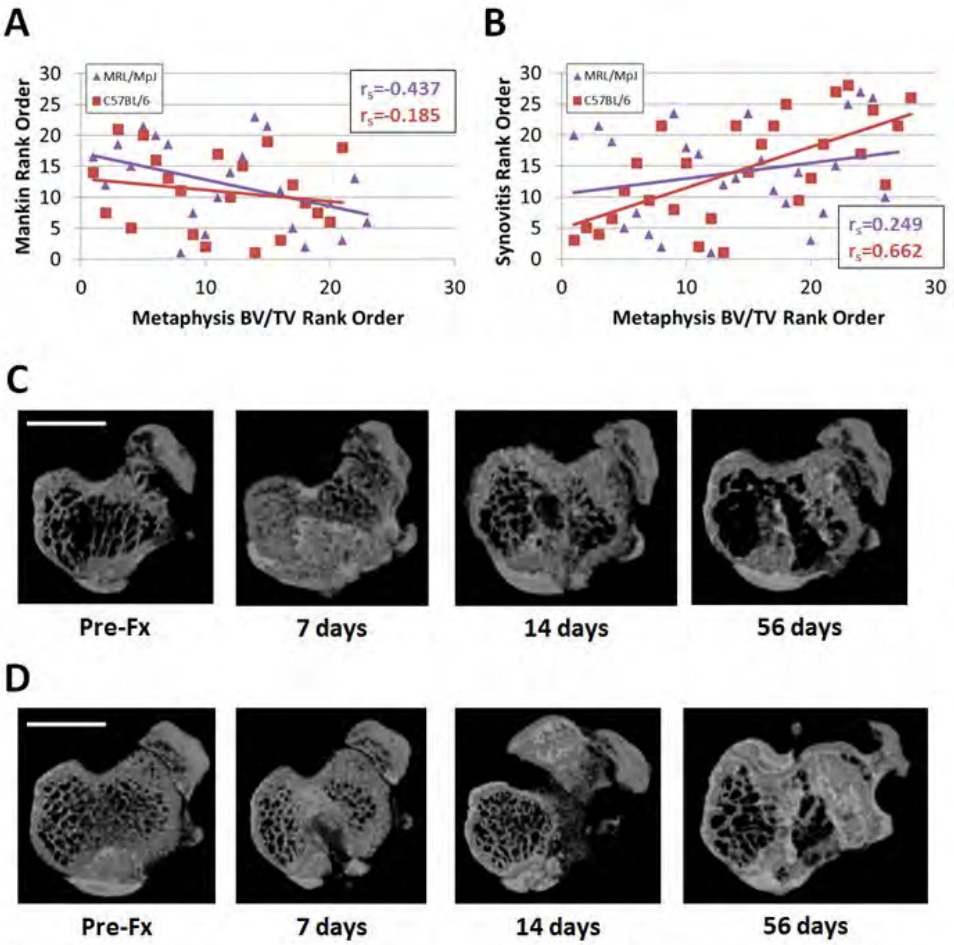

Figure 2

Correlations between Mankin total joint score, synovitis total joint score, and bone fraction (BV/TV) of the tibial metaphysis for both the MRL/MpJ and C57BL/6 strains. Values are displayed as a rank order within strain for each outcome measure (n=21-28 per strain). R_s values indicate Spearman correlation coefficient for each strain. **(A)** Mankin correlated with BV/TV (r_s=-0.437, p=0.0370) in the MRL/MpJ strain only. **(B)** Synovitis correlated with BV/TV (r_s=0.662, p=0.0001) in the C57BL/6 strain only. **(C)** Representative images of the tibial metaphysis for the C57BL/6 strain at each time point. Scale bar is 0.5mm. **(D)** Representative images of the tibial metaphysis for the MRL/MpJ strain at each time point. Scale bar is 0.5mm.

Novel In Vivo Micro-Computed Tomography Metrics of Joint Incongruity Predict Arthritis in a Knee Fracture Model

Tyler J. Vovos[1], Bridgette D. Furman, B.S.[1], Kelly A. Kimmerling, MEng[2], Gangadhar Utturkar[1], Louis E. DeFrate[1,2], Farshid Guilak[1,2], Steven A. Olson, MD[1].
[1]Duke University Medical Center, Durham, NC, USA, [2]Duke University, Durham, NC, USA.

Disclosures: T.J. Vovos: None. **B.D. Furman:** None. **K.A. Kimmerling:** None. **G. Utturkar:** 4; Teva Pharmaceutical Industries Ltd. **L.E. DeFrate:** 5; Arthrex, Cytex Therapeutics. **F. Guilak:** 3A; Cytex Therapeutics Inc.. 4; Cytex Therapeutics Inc.. 7; Elsevier Ltd. **S.A. Olson:** 3B; Bioventis. 5; Synthes USA, Bioventis.

Introduction: Post-traumatic arthritis (PTA) is an accelerated form of arthritis that develops following joint injury and occurs most predictably after intraarticular fracture [1, 2]. Joint degeneration may result from damage to the articular surface upon injury, or from residual joint instability or incongruity after injury [3]. Radiographic classification systems (e.g. Schatzker and AO/OTA) traditionally used to classify tibial plateau fracture severity do not account for 3D geometry of the joint surface [4]. A few research studies have used CT-based measures of joint fracture severity to predict PTA development [5]. To further characterize PTA development following joint trauma we developed a murine model of closed intraarticular fracture of the tibial plateau [6]. Interestingly, the MRL/MpJ "superhealer" strain of mice is protected from PTA following intraarticular fracture, thus providing valuable insight into the mechanical and inflammatory progression of PTA [7, 8]. Currently, the relationship between initial injury severity, articular surface displacement, and the development of PTA following intraarticular fracture in the MRL/MpJ and other mouse strains remains unknown. The objective of the current study was to develop in vivo micro-CT metrics of joint incongruity after intraarticular fracture to further characterize the pathomechanism of PTA. We hypothesized that quantitative measures of joint incongruity could be used to predict PTA development following intraarticular fracture. Furthermore, we hypothesized that the MRL/MpJ mouse would have an altered fracture healing response compared to the C57BL/6 mouse.
Methods: All animal procedures were performed in accordance with an IACUC-approved protocol. Skeletally mature male C57BL/6 (n=12, Charles River) and MRL/MpJ mice (n=12, Jackson Labs) were subjected to a closed intraarticular fracture (fx) (Fig 1) of the lateral tibial plateau using an established model [6, 9]. To generate similar fractures, indenter displacement was scaled relative to the size of the tibial plateau for each strain [7]. Fracture energy was calculated from the area under the load-displacement curve. At 8 weeks post-fx, all mice were sacrificed and arthritic changes in both fractured and non-fractured contralateral control knees were quantified using a modified Mankin score [6,10] of histologic sections (8 µm thick, FFPE, Safranin O/fast green). In vivo micro-CT (SkyScan 1176, Bruker) of fractured limbs was performed before and after fracture, and then at 1, 4, and 8 weeks post-fx. Bone surface deviations (BSD) were measured for all post-fx micro-CT scans. First, surface-rendered 3D digital models of the tibial plateau were generated from in vivo scans (CT-Analyser, Bruker). Models were then aligned to their respective pre-fx model's intact medial tibial plateau using an iterative closest point algorithm (Geomagic Studio, Geomagic®). BSDs were measured separately for the medial and lateral tibial plateau along three anatomic axes: antero-posterior (AP), latero-medial (LM), and axial (Geomagic

Control, Geomagic®). Positive and negative deviations of the bone surface were measured (Fig 1), and defined as the distance to a test surface (post-fx bone surface) that was either outside (positive) or inside (negative) of the reference surface (pre-fx bone surface). A deviation of 0% corresponded to perfect alignment of pre-fx and post-fx tibial plateaus. Color maps of BSDs were generated for each anatomical direction. An example of axial deviations in an MRL/MpJ mouse from post-fx to 8 weeks is shown in Fig 2.

Results: Intraarticular fractures were successfully created in all mice. Consistent with previous data [7], fracture energy was significantly greater for MRL/MpJ mice (148.1 ± 22.1 mJ) compared to C57BL/6 mice (106.6 ± 20.3 mJ) ($p<0.001$). Temporal patterns in BSDs were significantly different between C57BL/6 and MRL/MpJ mice over 8 weeks (Fig 2). Significant differences were observed in the lateral tibial plateau as measured by average positive axial deviation ($p = 0.01$), average positive LM deviation ($p = 0.015$), and maximum positive LM deviation ($p = 0.01$). Additionally, a significantly larger average positive axial deviation was observed in C57BL/6 mice at 8 weeks post-fx ($p=0.01$) (Fig 2). In the medial plateau, significant differences were seen between strains as measured by average positive axial deviation ($p=0.0487$) and average negative LM deviation ($p=0.0491$).

In assessing the relationship between BSDs of the joint after fracture and the development of PTA, total joint Mankin scores of degenerative changes were correlated to all BSDs measured in both mouse strains. Measures of BSDs from scans obtained immediately after fracture showed the strongest correlations with PTA development. In C57BL/6 mice, axial BSDs on post-fx day 0 were highly predictive of PTA severity at 8 weeks post-fx (Fig 3). In contrast, MRL/MpJ mice post-fx day 0 BSDs did not predict the development of PTA (Fig 3). Average positive AP deviation at the post-fx scan was also highly correlated to Mankin score in C57BL/6 mice ($R^2 =0.94$, $p=0.006$) but not in MRL/MpJ mice ($R^2 =0.25$, $p=0.10$).

Discussion: Through the development of novel in vivo micro-CT metrics of joint incongruity, we analyzed temporal patterns in bone surface deviations that revealed significant differences between C57BL/6 and MRL/MpJ strains over 8 weeks. Interestingly, after 8 weeks of fracture healing, we observed significantly larger bone surface deviations in C57BL/6 mice compared to MRL/MpJ mice. Furthermore, when applied to in vivo scans of the knee joint obtained immediately after fracture, our metrics of joint incongruity were capable of predicting the development of PTA in wild-type C57BL/6 mice, but not MRL/MpJ mice. These findings suggest that the MRL/MpJ strain undergoes a unique mechanism of fracture healing following intraarticular fracture, and that joint incongruities secondary to intraarticular fracture do not predispose MRL/MpJ mice to the development of PTA. Combined with an evolving knowledge of the biology of PTA development, our metrics hold potential as a tool for guiding PTA research in identifying physiologic processes that protect the MRL/MpJ strain from the effects of articular incongruity. Clinically, our metrics of joint incongruity could be used to predict which injuries are at risk for progression to PTA. Our observation that early measures of joint incongruity predict PTA in wild-type C57BL/6 mice corroborates previous findings that small articular incongruities after surgical fixation of intraarticular tibial plateau fractures predispose patients to the development of PTA [11]. Further, the translational potential of our joint incongruity metrics is high, as they could be readily applied to full scale clinical CT scans [12].

Significance: In vivo micro-CT metrics of joint incongruity provide a method for quantifying bone surface incongruities that have traditionally been difficult to measure and provide new possibilities to guide PTA

research and improve fracture management. The translational potential of our joint incongruity metrics is high, as they could readily be applied to full scale clinical CT scans.

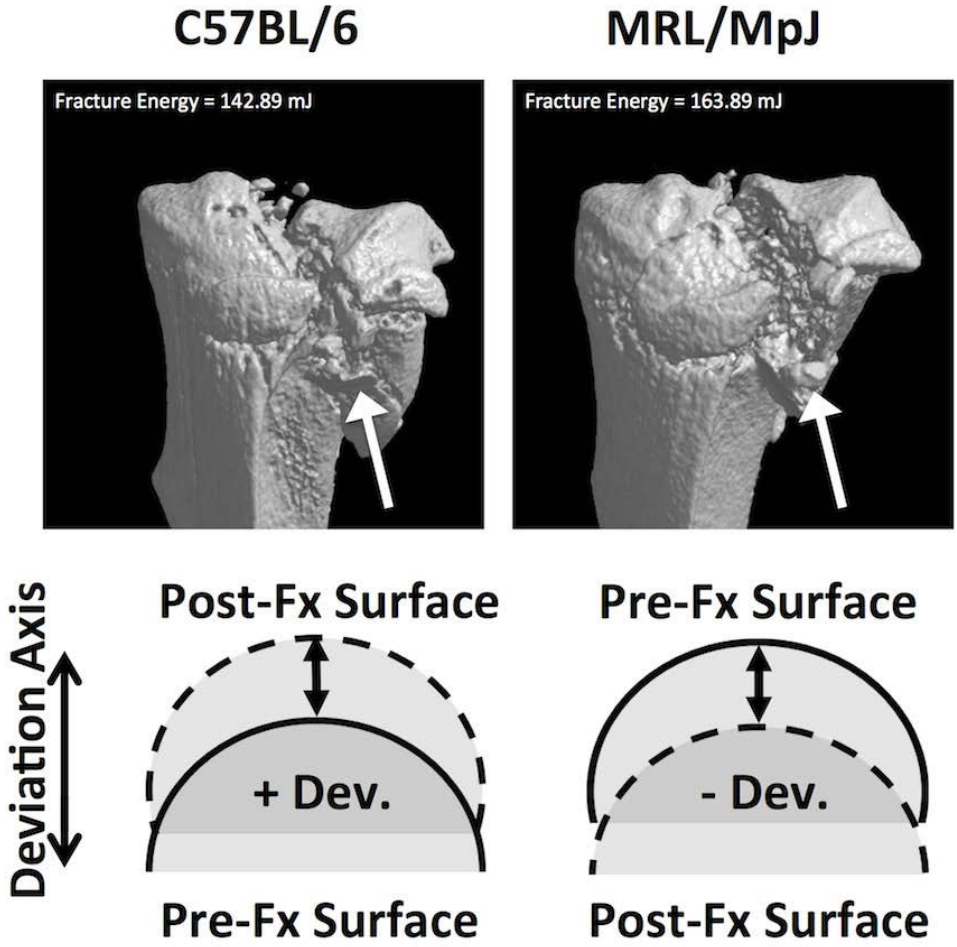

Figure 1. (Top) Micro-CT images of representative fractures. (Bottom) Metrics of joint incongruity after intra-articular fracture. Reference surface = pre-fracture; test surface = post-fracture.

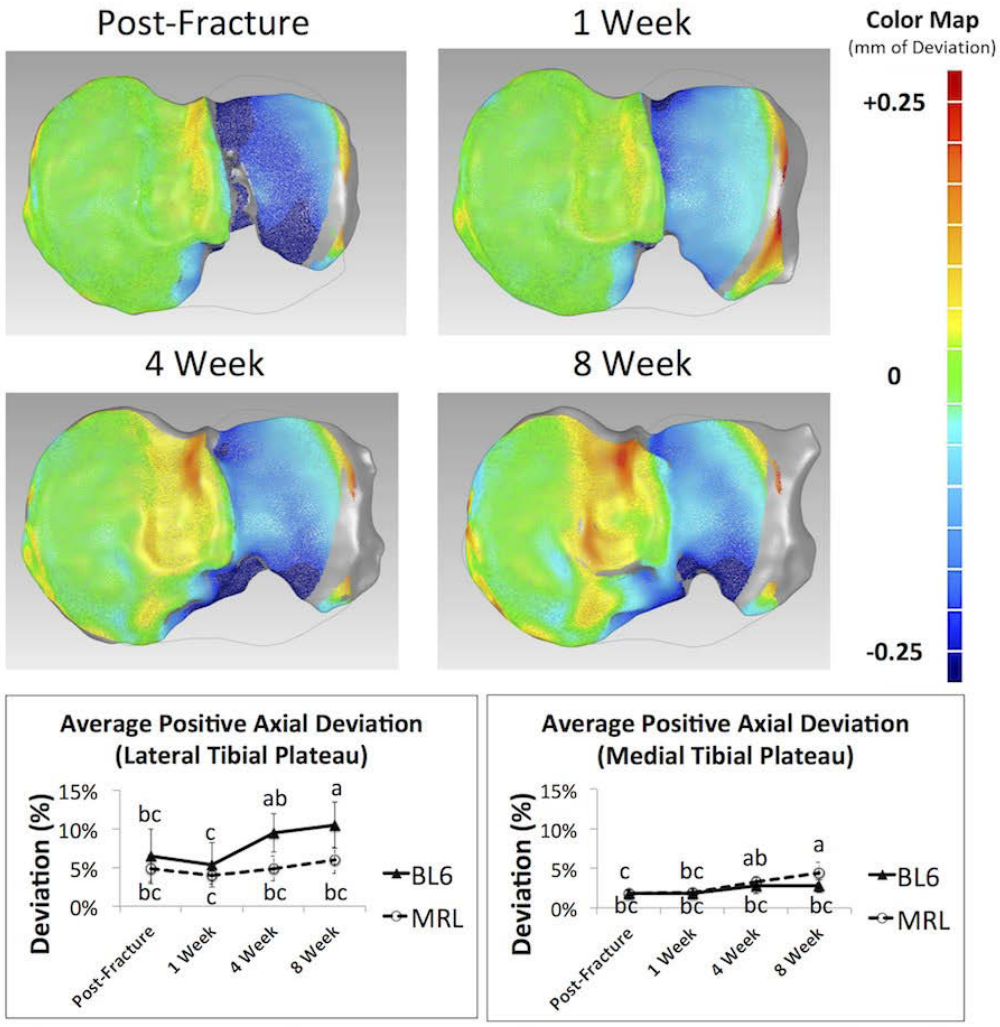

Figure 2. (Top) Representative color map of axial deviation with fracture healing. (Bottom) Significant strain-wise differences in fracture healing from post-fracture to 8 weeks.

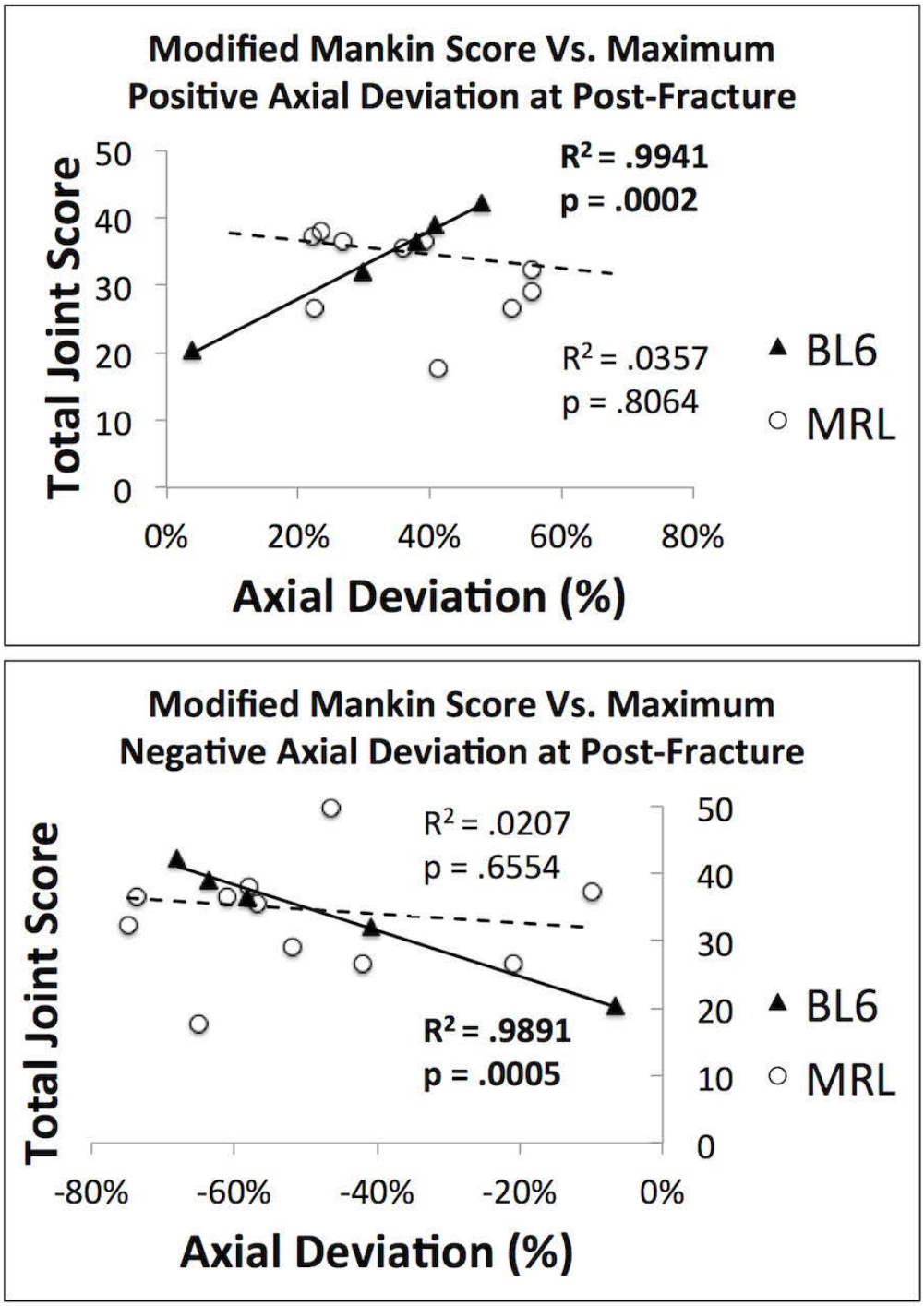

Figure 3. Correlations between total joint Mankin score for arthritis at 8 weeks post-fracture and post-fracture joint incongruity.

studied the correlation of sonographic measurements of the articular cartilage of the knee joint obtained from the posterolateral and posteromedial aspects to that obtained from the anterior aspect by the traditional method in patients with osteoarthritis of the knee.

Methods: We selected and studied the right knee of thirty one patients diagnosed with knee osteoarthritis, age ranging from 54 to 85 years who presented to our outpatient clinic. We used questionnaires to calculate Western Ontario and McMaster Ostoearthitis (WOMAC) scores and categorize patients into mild, moderate and severe osteoarthritis. and determined the correlation of the measurements to the severity of osteoarthritis. We excluded patients who could not extend the knee past 5 degrees or could not flex the knee beyond 135 degrees, patients with a knee effusion, and patients who had received an intra articular injection within the past month.

We measured the articular cartilage by the standard sonographic method using a GE Logiq e machine equipped with an 8-13 MHz linear transducer. We first measured cartilage thickness with the knee held in full flexion and at 140 degrees, at the medial and lateral aspects. We then measured the articular cartilage from the posterior aspect with the knee extended, over the medial and lateral condyles. We then compared the measurements obtained from the anterior aspect in full flexion to that obtained at 140 degrees and from the posterior aspect. We assumed a linear correlation between standard and posterior aspect measurements, hypothesized that a Pearson correlation coefficient greater than 0.77, corresponding to the lower bound of the 95% confidence interval of 0.6, would show satisfactory correlation between measurements.

Results: We demonstrated very good interobserver and intraobserver correlation between the two observers, with a correlation coefficient of 0.975 or higher at all sites. We compared the anterior and posterior measurements with Pearson correlation in both observers 1 and 2. Among the two observers, the greatest correlation for observer 1 was between the fully flexed anterolateral measurement to the posteromedial measurement with a Pearson correlation coefficient of 0.613, p-value = 0.000. Among measurements for observer 2, we found a Pearson correlation coefficient of 0.611, p-value = 0.000 between the fully flexed lateral and posteromedial measurements. We did not find correlation coefficients among the other measurements. We also noted that measurements from the posterior aspect appeared to be generally greater than those from the anterior aspect.

Conclusions: We did not find significant correlation between anterior and posterior measurements in patients with knee osteoarthritis. The highest correlation was found between anterolateral fully flexed and posteromedial measurements in both observers, with a Pearson correlation coefficient of 0.6. Posterior measurements, especially the posterolateral measurement appeared to be larger than anterior measurements indicating that posterior measurements of the articular cartilage by ultrasound may overestimate the cartilage measurements. We were unable to correlate the articular correlation with severity of osteoarthritis as majority of the patients had severe osteoarthritis (27/34 patients). Hence, although significant correlation between anterior and posterior measurements of the articular cartilage of the knee joint was observed in healthy volunteers, this was not the case in patients with osteoarthritis of the knee joint.

377
JOINT INCONGRUITY AND BIOMARKERS OF BONE METABOLISM AS PREDICTORS OF POST-TRAUMATIC ARTHRITIS IN MICE

T.J. Vovos †, B.D. Furman †, J.L. Huebner †‡, K.A. Kimmerling †§, G.M. Utturkar †, L.E. DeFrate †§, V.B. Kraus †‡, F. Guilak †§, S.A. Olson †.
† *Duke Univ. Med. Ctr., Durham, NC, USA;* ‡ *Duke Molecular Physiology Institute, Durham, NC, USA;* § *Duke Univ., Durham, NC, USA*

Purpose: Post-traumatic arthritis (PTA) develops predictably after articular fracture and may result from joint inflammation, hemarthrosis, or damage to the articular surface and residual joint instability or incongruity after injury. The MRL/MpJ "superhealer" mouse strain is protected from PTA and has reduced serum and synovial fluid levels of IL-1 and TNF-α acutely following fracture. The role of initial injury severity on PTA development following articular fracture is unclear. The objectives of this study were: 1) to measure acute and longitudinal displacement of the articular surface of the bone using in vivo microCT, and 2) to quantify serum bone markers following articular fracture. We hypothesized that quantitative measures of joint incongruity could predict PTA development and that MRL/MpJ mice would have an altered fracture healing response compared to C57BL/6 mice.

Methods: With an IACUC-approved protocol, male C57BL/6 and MRL/MpJ mice (n=12 each) were subjected to a closed articular fracture (fx) (Fig 1) of the lateral tibial plateau. Mice were sacrificed at 8wks post-fx, and arthritic changes were assessed in fractured and contralateral control knees (modified Mankin score). In vivo microCT was performed pre- and post-fx, and at 1, 4, and 8wks post-fx. Displacements of the articular surface of the bone, or Bone Surface Deviations (BSD), were quantified for the lateral and medial tibial plateau (Fig 1), defined as the displacement of the post-fx bone surface either outside (positive) or inside (negative) of the pre-fx bone surface (Fig 2). Blood was collected pre-fx, post-fx on day 4, and every 2wks to 6wks post-fx. Serum

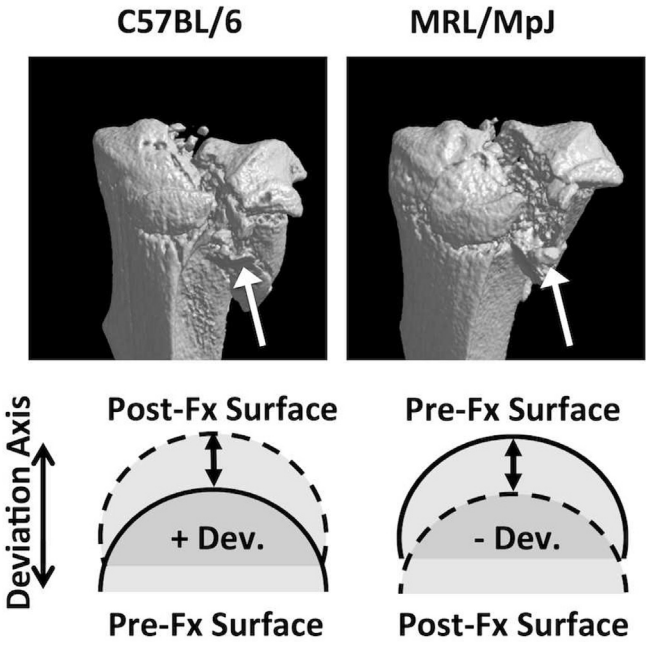

Figure 1(Top) Micro-CT images of representative fractures. (Bottom) Metrics of joint incongruity after intra-articular fracture. Reference surface = prefecture; test surface = post-fracture.

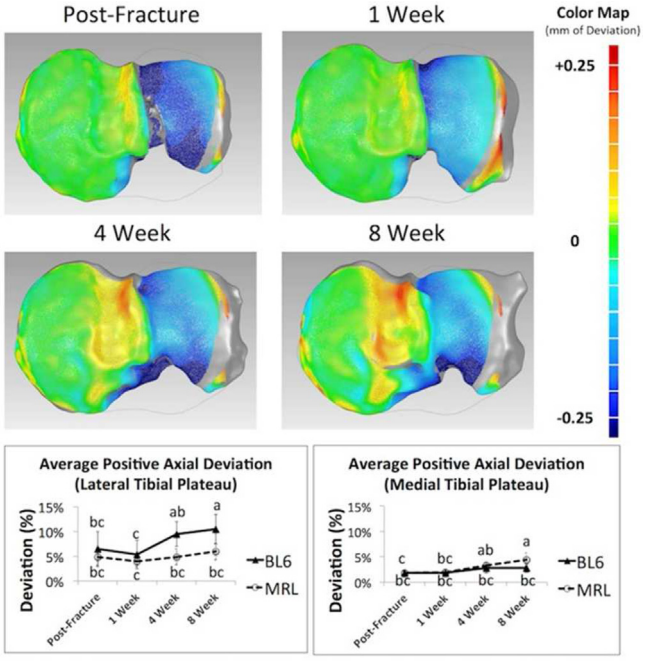

Figure 2(Top) Representative color map of axial deviation with fracture healing. (Bottom) Significant strain- wise differences in fracture healing to 8 weeks post- fracture *(data with different letters are significantly different).*

concentrations of biomarkers of bone metabolism were measured: procollagen type I N-propeptide (PINP), a bone formation marker; and C-terminal telopeptide of type I collagen (CTXI), a bone resorption marker. BSDs were analyzed using ANOVA. Bone marker concentrations were analyzed by Friedman test for repeated measures, and mouse strains were compared at each time point using the Holm-Sidak multiple t-test. Regression analysis was used to analyze the relationship between measured outcomes.

Results: Temporal patterns in BSDs were significantly different between C57BL/6 and MRL/MpJ mice with larger average positive axial deviations found in C57BL/6 mice at 8wks post-fx ($p=0.01$;Fig 2). Mankin scores were correlated to all BSDs in both mouse strains. Acute BSDs showed the strongest correlations with PTA development. In C57BL/6 mice, axial BSDs on post-fx day 0 were highly predictive of PTA severity at 8wks post-fx (Fig 3). In contrast, MRL/MpJ mice post-fx day 0 BSDs did not predict the development of PTA. Concentrations of PINP in the C57BL/6 mice were significantly lower than the MRL/MpJ mice post-fx ($p=0.005$;Fig 4), indicating a less robust acute bone anabolic response compared with the superhealer strain. Despite higher levels of CTXI in the C57BL/6 mice compared to the MRL/MpJ at pre-fx, no differences were found in CTXI levels post-fx between strains or at any time point.

Conclusions: Acute BSDs following articular fracture were predictive of arthritis development in C57BL/6 but not MRL/MpJ mice. C57BL/6 mice also showed an acute drop in serum PINP compared to MRL/MpJ mice. Larger BSDs were also observed in C57BL/6 mice compared to MRL/MpJ mice after 8 wks. Previous studies reported that C57BL/6 mice exhibit higher levels of inflammation post-fx than the MRL/MpJ mice and suggested that this may contribute to the development and progression of PTA in this model. This inflammatory environment may influence fracture healing immediately post-fx, potentially predisposing C57BL/6 mice to PTA. These findings suggest that joint incongruities secondary to articular fracture alone do not predispose mice to the development of PTA, but rather differences in bone metabolism may play a role in early healing, which may have a greater effect on outcome. Our results may provide insights into the physiologic processes determining PTA outcomes that may protect the MRL/MpJ strain from the effects of articular incongruity. Further, the translational potential of these incongruity metrics is high, as they could be readily applied to clinical CT scans.

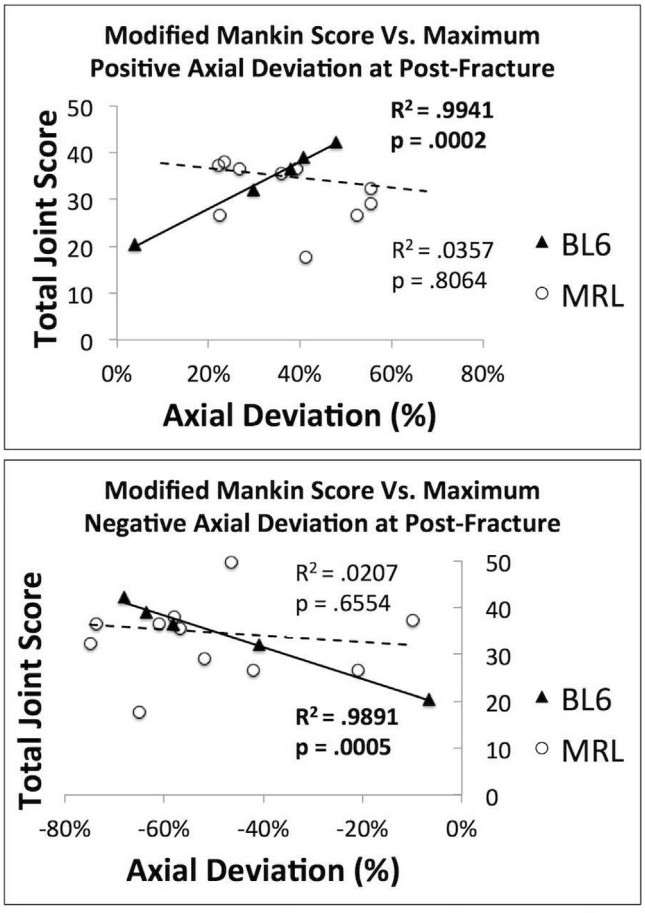

Figure 3. Correlations between total joint Mankin score for arthritis at 8 weeks post-fracture and post-fracture joint incongruity.

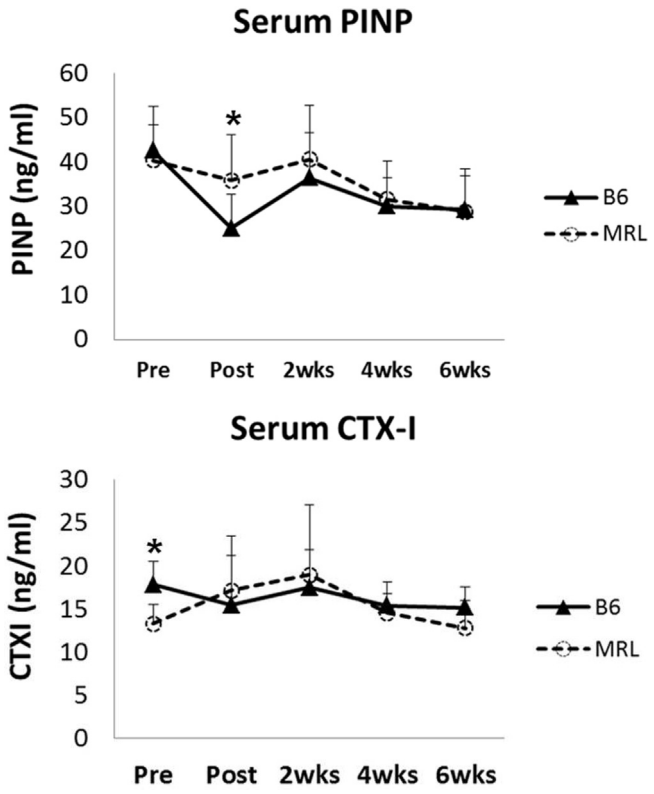

Figure 4. Serum concentrations of bone biomarkers PINP and CTX-I with articular fracture in C57BL/6 (B6) and MRL/MpJ (MRL) mice.

378

CLINICAL SIGNIFICANCE OF A KNEE EFFUSION DETECTED ON MRI BY MOAKS OR KIMRISS IN A PATIENT WITH KNEE OA

J.L. Jaremko, D. McDougall, B. Smith, R.G. Lambert, W.P. Maksymowych.
Univ. of Alberta, Edmonton, AB, Canada

Purpose: Presence of a joint effusion in knee osteoarthritis (OA) is thought to represent potentially treatable active inflammation. However, reliable assessment of presence and size of an effusion is surprisingly difficult. Effusions can be graded in a holistic fashion as present or absent, or by the MOAKS system which generates a whole-joint score from 0 (absent) to 3 (large). The volume of fluid can be directly measured by segmentation of T2-intense voxels, but this process requires workstation post-processing and some supervision. The KIMRISS semi-quantitative grading system offers an intermediate approach in which the width of joint fluid is measured and graded 0-3 in each of 4 standardized locations at the knee joint on axial and sagittal fluid-sensitive sequences, maximum score 12. The relative merits of each of these methods, and the clinical significance of detecting an effusion in a patient with knee OA, have been little studied. Accordingly, we used data from the Osteoarthritis Initiative to determine whether an effusion of different sizes detected by MOAKS or KIMRISS was associated with increased knee pain and disability at presentation or with an increased rate of use of intra-articular steroid injection over the next year.

Methods: Patients: This cohort study included knees from 40 subjects from the Osteoarthritis Initiative (OAI) that went on to have a knee steroid injection within 1 year of baseline evaluation, and 40 that did not, matched by age, sex, and Kellgren-Lawrence (K-L) grade of radiographic OA. Subjects averaged 62.3 years of age (range: 45-78), K-L grade 2.8±1.0 (mean±standard deviation), 78% were women, and body mass index (BMI) averaged 30.3±4.6. For each patient we extracted the

Assessment of Biomarkers Associated with Joint Injury and Subsequent Post-Traumatic Arthritis

PRORP: Translational Research Partnership Award / OR110100P1
W81XWH-12-1-0622

PI: Virginia B. Kraus **Org:** Duke University Medical Center **Award Amount:** $750,000

Study/Product Aim(s)

- The overall objective is to identify biomarkers following articular fracture that may be predictive of the development of post-traumatic arthritis (PTA).
- PTA is a severe burden in active duty and discharged soldiers. Compared to other forms of arthritis, PTA has a more rapid clinical onset. The goal of this work is to establish the basis for future use of biomarkers to predict the potential risk for developing PTA after acute joint injury.

Approach

- To accomplish this we will conduct a two part study:
- Biomarkers will be looked at in humans after knee joint fractures in biosamples (blood, synovial fluid, and urine) collected after injury. Special radiographic imaging will allow us to determine 18 months after injury which patients developed PTA from those who did not. We will then look for differences in biosamples between those with and without PTA.
- A companion series of animal experiments with two strains of mice will compare the human and mouse response following joint fracture. The low cost of mouse models lends itself to this type of work, and the results will provide a validated model for assessing future therapies to prevent PTA.

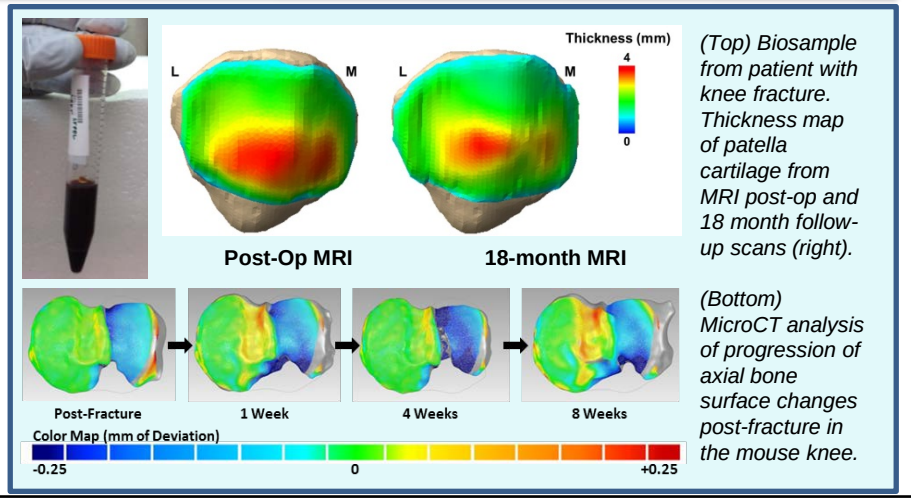

(Top) Biosample from patient with knee fracture. Thickness map of patella cartilage from MRI post-op and 18 month follow-up scans (right).

(Bottom) MicroCT analysis of progression of axial bone surface changes post-fracture in the mouse knee.

Accomplishments: Enrollment has closed with 20 patients enrolled in the study. Biosamples have been collected from all subjects and are stored for analyses. MRI scans are being obtained and analyzed. Mice microCT analysis is near completion, and histology is underway.

Timeline and Cost

Activities CY	13	14	15	16*
Enroll knee fracture patients, collect biosamples, initial MRI				
Create articular fracture in knee of mice and harvest samples				
Analysis of mice samples, and obtain MRI at 18 months.				
Analyze biosamples and compare human data to mice				
Estimated Budget ($K)	**$238**	**$233**	**$279**	**NCE***

***No Cost Extension (NCE)**

Updated: 30 October 2015

Goals/Milestones

CY13 Goals – *Begin patient biosample collection, MRI scans, and animal studies*

☑ Obtained IRB approval of human use in study, enrolled 9 patients, processed and stored biosamples, and obtained initial MRI scans.

☑ Obtained IACUC approval for animal use in study, created fractures in mice, and harvested samples for early time points.

CY14 Goals – *Continue patient biosample collection, MRI scans, and animal studies*

☑ Enrolled 9 additional patients, collected biosamples, obtained initial MRI scans, and collected 18 month follow-up MRI scans from first two patients.

☑ Created fractures in mice, harvested samples, started microCT and histologic analysis.

CY15 Goal – *Biomarker analyses of human and mouse samples*

☑ Perform assays to measure biomarkers and proteomics analysis.

☑ Complete animal study histology, microCT analysis.

☐ Complete statistical analyses of proteomics and analyses of follow-up MRI scans.

☐ Complete animal and human biomarker assays and compare.

Comments/Challenges/Issues/Concerns

- Patient enrollment was initially slow, and we have received a one year no cost extension in order to complete all MRI, biomarker, and proteomic analyses.
- Due to slow enrollment, some expenditures have been delayed. However, the year to date and cumulative balances do not exceed 25% of the projected budget.

Budget Expenditure to Date:

Year 3: Projected-$279K Actual-$239K; Cumulative: Projected-$750K Actual-$628K